A Harmonic Field Model of Consciousness in the Human Brain

Lee Smart[1,**]

[1] Independent Researcher, Vibrational Field Dynamics Project
Twitter/X: @vfd_org
contact@vibrationalfielddynamics.org

Abstract

Traditional approaches to the neural correlates of consciousness emphasize spectral power in discrete frequency bands, yet this framework fails to explain key empirical puzzles—most notably, the coexistence of strong delta activity with conscious experience. We present a harmonic field model that reconceptualizes brain activity as a spatially distributed field expanded in connectome harmonics: the unique eigenmodes of the graph Laplacian derived from structural connectivity. This harmonic basis is not a modeling choice but a mathematical consequence of network structure. Neural dynamics are governed by coupled second-order equations for mode amplitudes, linking spatial (eigenvalue-based) and temporal (frequency-based) properties within a unified formalism. We define a consciousness functional that combines five components—mode entropy, participation ratio, phase coherence, entropy production rate, and criticality index—to quantify the degree of consciousness supported by a given field configuration. This functional depends on the global distribution and dynamics of mode amplitudes rather than power in any single frequency band. We demonstrate that the model resolves the delta paradox: states with high delta power can exhibit high or low consciousness depending on mode diversity, coherence, and proximity to criticality. The framework generates testable predictions for sleep, anesthesia, psychedelics, and disorders of consciousness, and provides a principled bridge between empirical neuroscience and geometric field theories. By shifting focus from frequency bands to field configurations, the harmonic model offers a mathematically rigorous, empirically grounded approach to understanding how the brain generates conscious experience.

**Corresponding author. Email: contact@vibrationalfielddynamics.org

1 Introduction

The search for the neural correlates of consciousness has been a central endeavor of modern neuroscience. Over the past several decades, researchers have accumulated substantial evidence linking specific patterns of brain activity to conscious experience, identifying neural signatures that distinguish wakeful awareness from sleep, anesthesia, and pathological states of impaired consciousness [1, 2]. Yet despite this progress, a unified theoretical framework that explains *why* certain neural configurations support consciousness while others do not remains elusive. The field has accumulated correlations without a principled account of the underlying mechanism.

A prominent approach has been to characterize consciousness in terms of neural oscillations—the rhythmic fluctuations in electrical activity observed across the brain. Electroencephalography (EEG) and magnetoencephalography (MEG) reveal a rich spectral structure, traditionally decomposed into frequency bands: delta (1–4 Hz), theta (4–8 Hz), alpha (8–13 Hz), beta (13–30 Hz), and gamma (30–100 Hz) [3]. Different bands have been associated with different cognitive functions and states of consciousness. Alpha rhythms are linked to relaxed wakefulness, gamma oscillations to perceptual binding and attention, and delta waves to deep sleep [4, 5, 6].

1.1 Limitations of Band-Based Thinking

While the frequency-band framework has proven useful for descriptive purposes, it suffers from several conceptual and empirical limitations:

1. **Arbitrary boundaries.** The division into discrete bands is conventional rather than principled. There is no sharp physiological transition at 4 Hz or 13 Hz; the boundaries are historical artifacts that obscure the continuous nature of the spectrum.

2. **Conflation of spatial and temporal structure.** A given frequency can arise from very different spatial configurations of neural activity. Delta power, for instance, can reflect globally synchronized slow waves or local, asynchronous fluctuations. Band power alone does not distinguish these cases.

3. **Inconsistent correlations.** The relationship between frequency bands and consciousness is not uniform. Alpha power can increase or decrease with attention depending on context; gamma activity is present in both conscious perception and unconscious processing [7]. No single band reliably indexes consciousness.

4. **The delta paradox.** Most strikingly, the association between delta activity and unconsciousness—while statistically robust—admits important exceptions. Dreams occur during non-REM (NREM) sleep despite prominent delta waves [8]; certain meditative states feature enhanced slow oscillations alongside vivid awareness [9]; and patients occasionally report conscious experience during anesthesia despite delta-dominated EEG [10]. These observations challenge the assumption that delta activity is intrinsically incompatible with consciousness.

The delta paradox, in particular, reveals the inadequacy of band-based thinking. If consciousness were simply a function of spectral power in various bands, the coexistence of strong delta activity with conscious experience would be inexplicable. Something beyond frequency content must determine whether a brain state supports consciousness.

1.2 The Need for a Unified Harmonic/Field Model

We propose that the resolution lies in shifting from a band-based to a *field-based* perspective. Rather than asking "how much delta, alpha, or gamma power is present?" we ask "what is the overall configuration of the brain's activity field, and what are its dynamical and statistical properties?"

This shift is motivated by several considerations:

1. **The brain as a spatially extended system.** Neural activity is not a collection of independent oscillators but a spatially distributed field constrained by the brain's structural connectivity. The white-matter architecture defines a network over which activity propagates and interacts. Any adequate model must account for this spatial structure.

2. **Connectome harmonics.** Recent work has shown that the brain's structural connectivity defines a natural basis of spatial patterns—the eigenmodes of the graph Laplacian derived from the connectome [11, 12]. These "connectome harmonics" are the graph-theoretic analogues of Fourier modes or spherical harmonics, providing a principled decomposition of brain activity into spatially coherent patterns. Importantly, this basis is not one choice among many—it is the unique eigenbasis of the connectivity operator, making harmonic decomposition a mathematical necessity rather than a modeling preference.

3. **Field dynamics.** The temporal evolution of neural activity can be described by dynamical equations acting on this spatial field. By pro-

jecting onto the harmonic basis, the field dynamics reduce to a system of coupled equations for the mode amplitudes—a mathematically tractable representation of large-scale brain dynamics.

4. **Consciousness as field configuration.** If consciousness depends on the global organization of brain activity, then it should be characterized not by the power in isolated frequency bands but by properties of the full mode distribution: its entropy, its coherence, its dynamical regime. This perspective naturally accommodates the delta paradox, since a state can have high delta power (strong low-frequency modes) while still exhibiting the complexity, integration, and criticality associated with consciousness.

1.3 Contributions of This Paper

In this paper, we develop a *harmonic field model of consciousness* that formalizes these ideas. Our contributions are as follows:

1.3.1 Brain-as-Field Formalism Using Connectome Harmonics

We represent the brain's structural connectivity as a weighted graph $G = (V, E)$ with adjacency matrix A and graph Laplacian $L = D - A$. The eigenmodes ψ_k of the Laplacian, satisfying $L\psi_k = \lambda_k \psi_k$, define the connectome harmonics—a complete orthonormal basis for spatial patterns of activity. Time-varying neural activity $X(t)$ is expanded as

$$X(t) = \sum_{k=1}^{N} a_k(t)\, \psi_k, \tag{1}$$

where the mode amplitudes $a_k(t)$ capture the instantaneous contribution of each harmonic. This representation reframes brain activity as a superposition of standing waves shaped by anatomy.

1.3.2 Dynamical Model for Mode Amplitudes

We specify a second-order dynamical equation for the neural activity field and project it onto the harmonic basis to obtain equations for the mode amplitudes:

$$\ddot{a}_k(t) + \gamma_k \dot{a}_k(t) + \omega_k^2 a_k(t) + \frac{\partial U}{\partial a_k}(a_1, \ldots, a_N) = I_k(t) + \xi_k(t). \tag{2}$$

Here, γ_k is a damping coefficient, ω_k is the natural frequency of mode k, U is a nonlinear coupling potential, I_k is external input, and ξ_k is noise. This system of coupled, damped, driven oscillators provides a tractable model of large-scale brain dynamics, connecting structural (eigenvalue-based) and temporal (frequency-based) properties.

1.3.3 Consciousness Functional $C(t)$

We define a scalar functional $C(t)$ that quantifies the degree of consciousness supported by a given harmonic field configuration. This functional combines five components:

- **Mode entropy** $H_{\text{mode}}(t) = -\sum_k p_k(t) \log p_k(t)$, measuring the diversity of power distribution across modes.
- **Participation ratio** $\text{PR}(t) = 1/\sum_k p_k(t)^2$, estimating the effective number of active modes.
- **Phase coherence** $R(t) = |\frac{1}{N}\sum_k e^{i\theta_k(t)}|$, capturing synchronization among modes.
- **Entropy production rate** $\dot{S}(t)$, quantifying non-equilibrium drive.
- **Criticality index** $\kappa(t)$, measuring proximity to a dynamical phase transition.

The combined functional is

$$C(t) = \alpha \frac{H_{\text{mode}}(t)}{H_{\max}} + \beta \frac{\text{PR}(t)}{\text{PR}_{\max}} + \gamma R(t) + \delta \frac{\dot{S}(t)}{\dot{S}_{\max}} + \varepsilon \kappa(t), \tag{3}$$

with positive weights $\alpha, \beta, \gamma, \delta, \varepsilon$. This functional synthesizes insights from information theory, dynamical systems, non-equilibrium thermodynamics, and synchronization theory into a unified measure.

1.3.4 Resolution of the Delta Paradox

The harmonic field model resolves the delta paradox by showing that delta power reflects the activation of low-index, spatially global modes, while consciousness depends on the *overall configuration* of the mode distribution. A state can have high delta power yet still exhibit high mode entropy, participation ratio, coherence, entropy production, and criticality—yielding a high $C(t)$. Conversely, a state can have high delta power with collapsed

diversity and criticality, yielding low $C(t)$. The paradox dissolves once we recognize that frequency bands are spectral signatures of the field state, not determinants of consciousness.

1.3.5 Framework for Integrating Deeper Geometric Field Theories

Finally, we show that the harmonic field model is compatible with a broad class of underlying geometric and field-theoretic frameworks. The graph Laplacian can be viewed as a discrete approximation to a Laplace–Beltrami operator on an effective manifold; the mode dynamics have the same form as field equations expanded in a spectral basis. This positions the model as a bridge between empirical neuroscience and more fundamental physical descriptions, without committing to any specific underlying theory.

1.4 Outline of the Paper

The remainder of this paper is organized as follows:

- **Section 2** introduces the brain as a harmonic field medium, defining the graph Laplacian, its eigenmodes, and the harmonic expansion of neural activity.
- **Section 3** develops the dynamical equations for mode amplitudes, including the stochastic Ornstein–Uhlenbeck approximation and the relationship to EEG frequency bands.
- **Section 4** defines the consciousness functional $C(t)$, specifying each component and discussing its relationship to existing measures.
- **Section 5** applies the model to resolve the delta paradox, providing mathematical illustrations and case analyses across sleep, anesthesia, and altered states.
- **Section 6** discusses the compatibility of the model with geometric field theories, emphasizing its role as a bridge to deeper physical descriptions.
- **Section 7** summarizes the contributions, discusses limitations, and outlines directions for future research.
- **Appendix A** provides detailed mathematical derivations and alternative formulations.

1.5 Scope and Epistemological Stance

We emphasize that the harmonic field model is a *formal framework* for describing consciousness in terms of brain dynamics, not a claim to have solved the "hard problem" of consciousness—the question of why physical processes give rise to subjective experience at all [13]. Our goal is more modest: to provide a mathematically rigorous, empirically testable model that captures the *neural correlates* of consciousness in a principled way, resolves empirical puzzles like the delta paradox, and interfaces smoothly with both neuroscientific data and more fundamental physical theories.

The model makes quantitative predictions testable against EEG, MEG, and fMRI data from subjects in various states of consciousness. It provides a vocabulary for comparing and integrating existing measures of neural complexity and consciousness, and it suggests new directions for both experimental and theoretical research. Whether consciousness is ultimately reducible to harmonic field configurations or whether deeper explanations are required, the framework developed here offers a productive step toward a unified understanding of how the brain generates conscious experience.

Recent Advances and Converging Evidence

Several recent developments in systems and cognitive neuroscience indicate a growing shift toward multiscale and integrative accounts of neural computation and conscious experience. For example, recent reviews have reframed mixed selectivity and population coding as dynamic gating processes in which oscillations and neuromodulatory context determine which variable combinations are transmitted forward for readout [14]. This perspective emphasizes high-dimensional representational flexibility emerging from structured, oscillation-dependent interactions among distributed neural populations.

Parallel lines of research on sleep, dreaming, and anesthesia increasingly demonstrate that consciousness can persist under delta-rich or slow-wave conditions, provided that certain global integrative structures are preserved [15]. These findings challenge frequency-band interpretations that equate low-frequency dominance with unconsciousness and instead support models in which state differences depend on global patterns of neural interaction rather than on spectral content alone.

At the same time, advances in connectome harmonics and network-mode analyses highlight that structured graphs—whether anatomical or effective connectivity networks—naturally support a hierarchy of eigenmodes that

organize large-scale neural activity [11, 16]. Combined, these developments point toward a consensus that global configuration, high-dimensional interactions, and network-constrained dynamics are essential for understanding conscious states. The harmonic-field model developed in this work provides a mathematically explicit formulation of this emerging paradigm.

Mixed Selectivity as Oscillatory Gating: Implications for the Harmonic Field Model

A particularly important development for the present framework is the reconceptualization of mixed selectivity in neural populations [17]. Mixed selectivity—the property whereby individual neurons respond to nonlinear combinations of task-relevant variables—has long been recognized as essential for flexible, high-dimensional population codes that support complex cognition. Recent work has clarified the mechanism: oscillatory phase and neuromodulatory context dynamically determine which features are mixed and which combinations can reach downstream readout circuits. Rather than being a static property of neural tuning, mixed selectivity emerges from time-varying gating operations governed by oscillatory dynamics.

This oscillatory gating perspective maps naturally onto the harmonic field framework. In the present model, each connectome harmonic ψ_k defines a spatial pattern of coordinated activity, and the mode amplitude $a_k(t)$ determines its instantaneous contribution. Oscillatory gating, in this view, corresponds to the selective activation of specific harmonic modes: when certain modes are energized and phase-aligned, their associated spatial patterns combine to produce high-dimensional mixed representations. Low-index modes, which engage broad cortical territories, correspond to globally broadcast variables; mid- and high-index modes, with finer spatial structure, implement local nonlinear combinations. The phase relationships among modes thus determine which variable combinations can be read out by downstream circuits.

This correspondence suggests that the harmonic field model provides a principled geometric substrate for the dynamic gating mechanisms described in recent population coding work. The mode structure is not arbitrary but is determined by the brain's structural connectivity; the gating rules emerge from the dynamics governing mode amplitudes and phases. In the sections that follow, we develop this correspondence formally, showing how mode entropy, participation ratio, and phase coherence jointly capture the conditions under which flexible, high-dimensional representations can support conscious processing.

Code and Data Availability. A public code and figure-generation repository accompanying this paper is available at:
`https://github.com/vfd-org/harmonic-field-consciousness`

2 Brain as a Harmonic Field Medium

The central premise of this work is that the brain can be fruitfully modeled as a harmonic field medium—a spatially extended system whose activity is naturally decomposed into a basis of standing waves determined by its structural connectivity. This perspective shifts attention away from localized neural activations toward global patterns of coordinated activity, providing a principled mathematical framework for understanding large-scale brain dynamics.

2.1 The Structural Connectome as a Graph

We begin by representing the brain's white-matter architecture as a graph $G = (V, E)$, where V is a set of N nodes (cortical and subcortical regions) and E is a set of edges encoding structural connections between them [18, 19]. The choice of parcellation—whether into hundreds or thousands of regions—determines the resolution of the model, but the formalism remains general.

Each edge $(i, j) \in E$ carries a weight $w_{ij} \geq 0$ reflecting the strength of the anatomical connection, typically estimated from diffusion-weighted MRI tractography as the number or density of streamlines connecting regions i and j [20]. These weights populate the *adjacency matrix* $A \in \mathbb{R}^{N\times N}$, a symmetric matrix with entries

$$A_{ij} = \begin{cases} w_{ij} & \text{if } (i,j) \in E, \\ 0 & \text{otherwise.} \end{cases} \tag{4}$$

For the present treatment we assume $A_{ii} = 0$ (no self-loops), though extensions incorporating local recurrence are straightforward.

The *degree matrix* $D \in \mathbb{R}^{N\times N}$ is diagonal, with entries

$$D_{ii} = \sum_{j=1}^{N} A_{ij}, \tag{5}$$

representing the total connection strength of node i. The *graph Laplacian* is then defined as

$$L = D - A. \tag{6}$$

This matrix is symmetric and positive semi-definite, with a zero eigenvalue corresponding to the constant eigenvector when the graph is connected. The Laplacian encodes how activity at each node relates to activity at its neighbors: $(L\mathbf{x})_i = D_{ii}x_i - \sum_j A_{ij}x_j$ measures the deviation of node i from the weighted average of its neighbors.

2.2 Eigenmodes of the Graph Laplacian

Because L is real and symmetric, it admits a complete orthonormal eigenbasis. Solving the eigenproblem

$$L\psi_k = \lambda_k \psi_k, \quad k = 1, \ldots, N, \tag{7}$$

yields eigenvalues $0 = \lambda_1 \leq \lambda_2 \leq \cdots \leq \lambda_N$ and corresponding eigenvectors $\psi_k \in \mathbb{R}^N$, normalized so that $\psi_k^T \psi_j = \delta_{kj}$.

These eigenvectors are the *connectome harmonics*—the natural modes of oscillation supported by the brain's structural network [11, 12]. They are the graph-theoretic analogues of Fourier modes on a continuous domain or spherical harmonics on a sphere. The associated eigenvalue λ_k quantifies the spatial frequency of mode k: low-λ modes vary smoothly across the network, engaging large, contiguous communities of regions, while high-λ modes exhibit rapid spatial variation and fine-grained structure. Fig. 1 illustrates this progression on a toy graph.

Crucially, this harmonic decomposition is not one of many possible bases—it is the unique eigenbasis of the connectivity operator. Any network with a well-defined Laplacian admits exactly this decomposition; the harmonic basis is therefore not a modeling choice but a mathematical consequence of structured connectivity.

Several properties of this spectral decomposition merit emphasis:

1. **Smoothness and spatial scale.** The first nontrivial eigenmode ψ_2 (the Fiedler vector) partitions the network into two communities with minimal cut, capturing the coarsest spatial contrast [21]. Successive modes introduce progressively finer subdivisions.

2. **Completeness.** Any pattern of activity over the N nodes can be exactly represented as a linear combination of the N eigenmodes. No information is lost in projecting onto this basis.

3. **Anatomical grounding.** Unlike Fourier modes on a regular grid, connectome harmonics are shaped by the idiosyncratic geometry and

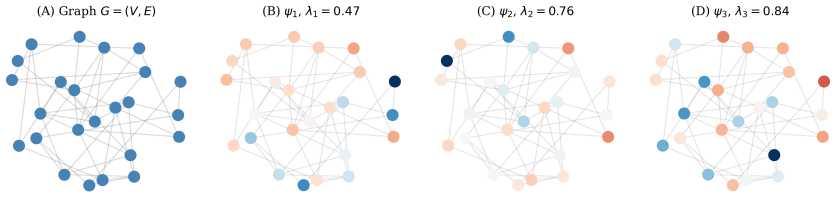

Figure 1: Visualization of the first three harmonic modes on a toy graph. (A) The graph structure $G = (V, E)$, a 24-node small-world network. (B–D) The first three nontrivial Laplacian eigenmodes ψ_1, ψ_2, ψ_3, with nodes colored by mode amplitude (red positive, blue negative). Low-index modes capture coarse spatial structure; higher modes exhibit progressively finer patterns.

topology of the brain's wiring. They respect anatomical boundaries and long-range projections.

4. **Invariance.** For a fixed parcellation and tractography, the eigenmodes are structural invariants of the individual brain. They provide a canonical coordinate system for describing time-varying activity.

Empirical studies have demonstrated that resting-state fMRI activity preferentially occupies low-frequency connectome harmonics, suggesting that the brain's spontaneous dynamics are constrained by its structural eigenmodes [11, 16].

2.3 Neural Activity as a Field

We now introduce a time-dependent *neural activity field* $X(t) \in \mathbb{R}^N$, where $X_i(t)$ represents the aggregate activity of region i at time t. Depending on the measurement modality, $X_i(t)$ may correspond to the BOLD signal (fMRI), the local field potential (intracranial EEG), the electric or magnetic field (scalp EEG/MEG), or a more abstract measure such as firing rate averaged over a neuronal population.

Because the eigenmodes $\{\psi_k\}_{k=1}^N$ form a complete orthonormal basis for $\mathbb{R}^N$, we can expand $X(t)$ as

$$X(t) = \sum_{k=1}^{N} a_k(t)\, \psi_k, \tag{8}$$

where the *mode amplitudes* $a_k(t) = \psi_k^T X(t)$ are the projections of the instantaneous activity onto each eigenmode. This decomposition is exact and invertible: given $\{a_k(t)\}$, we recover $X(t)$ via Eq. (8); given $X(t)$, we obtain $a_k(t)$ by projection.

The representation (8) reframes brain activity as the superposition of standing waves, each with a characteristic spatial pattern ψ_k and a time-varying amplitude $a_k(t)$. In this view, the brain is a resonant medium in which structural connectivity determines which patterns are geometrically privileged, while dynamics select which modes are energized at any moment.

2.4 Interpretation as Standing Waves

The analogy to standing waves in physical media is more than metaphorical. Consider a vibrating membrane or an acoustic cavity: the spatial eigenmodes are determined by the geometry and boundary conditions, and the temporal evolution of each mode is governed by a wave equation with mode-specific frequency. In the brain, the graph Laplacian plays the role of the spatial operator, and the eigenvalues λ_k are related to the natural frequencies of the modes.

To make this precise, suppose the dynamics of $X(t)$ are approximately governed by a wave-like equation of the form

$$\ddot{X}(t) = -\Omega^2 L\, X(t) + (\text{damping, nonlinearity, input, noise}), \tag{9}$$

where Ω sets an overall frequency scale. Substituting the expansion (8) and using the eigenvalue equation (7), we obtain decoupled equations for each mode amplitude:

$$\ddot{a}_k(t) = -\Omega^2 \lambda_k\, a_k(t) + \cdots \tag{10}$$

Thus $\omega_k = \Omega\sqrt{\lambda_k}$ serves as the natural angular frequency of mode k in the absence of damping and coupling. Low-eigenvalue modes oscillate slowly; high-eigenvalue modes oscillate rapidly. This mapping provides a bridge between the structural (spectral) and temporal (oscillatory) properties of brain activity, a theme we develop fully in Section 3.

The standing-wave picture also clarifies the relationship between spatial scale and temporal frequency. Low-frequency oscillations (e.g., delta, theta) are dominated by low-index modes that engage broad swathes of cortex, while high-frequency oscillations (e.g., gamma) reflect high-index modes with fine spatial structure. This is consistent with empirical observations that slow oscillations tend to be globally coherent, whereas fast oscillations are more spatially localized [3, 22].

This framework also illuminates the role of oscillatory phase in gating neural computations. Recent work on mixed selectivity has shown that oscillatory phase determines which combinations of variables reach downstream readout circuits [17]. In the harmonic model, each mode ψ_k carries both a spatial signature and a phase $\theta_k(t)$. The phase relationships among modes determine which harmonic combinations are functionally active at any instant: when modes are phase-aligned, their contributions sum constructively and can influence downstream processing; when out of phase, they cancel or remain functionally segregated. Oscillatory gating, in this view, is implemented through mode-phase coordination, with the harmonic basis providing the structured substrate on which gating operations act.

Recent work on mixed selectivity has clarified that population codes dynamically reconfigure depending on oscillatory phase, neuromodulatory tone, and local circuit state. In this view, oscillations do not "carry" information directly; they act as gating variables that select which combinations of features can reach downstream readout circuits. The harmonic framework provides an immediate geometric substrate: each ψ_k defines a structured spatial pattern, and oscillatory gating corresponds to selective activation and phase-alignment among these harmonics. When multiple modes become conjunctively active, their nonlinear combinations implement high-dimensional mixed-selectivity codes. Thus, the connectome harmonic structure provides the anatomical coordinate system in which oscillatory gating naturally operates.

2.5 Relationship to Electromagnetic Fields

Neural activity is inherently electromagnetic. Action potentials and synaptic currents generate electric and magnetic fields that superpose throughout brain tissue and can be measured at the scalp (EEG, MEG) or intracranially [23, 24]. The neural activity field $X(t)$ defined above is intimately related to the sources of these electromagnetic signals.

In the forward model of EEG/MEG, the measured signal $Y(t)$ at sensor locations is a linear transformation of the source activity:

$$Y(t) = M\,X(t) + \epsilon(t), \tag{11}$$

where M is a lead-field matrix encoding the propagation of electric or magnetic fields from sources to sensors, and $\epsilon(t)$ is measurement noise. Substi-

tuting the harmonic expansion (8), we obtain

$$Y(t) = \sum_{k=1}^{N} a_k(t)\,(M\psi_k) + \epsilon(t). \tag{12}$$

Each connectome harmonic ψ_k has a corresponding scalp topography $M\psi_k$, and the measured signal is the amplitude-weighted superposition of these topographies.

This formulation has practical implications for source reconstruction. Rather than estimating the full N-dimensional source vector $X(t)$, one can estimate the lower-dimensional mode amplitudes $a_k(t)$, exploiting the smoothness prior implicit in the harmonic basis [11]. It also suggests that the classical EEG frequency bands (delta, theta, alpha, beta, gamma) are emergent spectral signatures of the underlying harmonic dynamics, not fundamental categories in themselves—a point central to our resolution of the delta paradox in Section 5.

Beyond measurement, there is growing interest in whether endogenous electromagnetic fields play a functional role in brain dynamics, perhaps through ephaptic coupling or field-mediated integration [25, 26]. In such scenarios, the connectome harmonics could serve as the natural modes of the brain's electromagnetic field, with the field itself acting as a substrate for large-scale integration. While our primary focus is on the formal structure of the harmonic model, we note its compatibility with these electromagnetic field theories of consciousness.

2.6 Summary

In this section we have established the mathematical foundations of the harmonic field model:

- The brain's structural connectivity is represented as a weighted graph $G = (V, E)$ with adjacency matrix A and graph Laplacian $L = D - A$.
- The Laplacian eigenmodes ψ_k and eigenvalues λ_k define the connectome harmonics—a complete, orthonormal basis of standing-wave patterns shaped by anatomy.
- Time-varying neural activity $X(t)$ is expanded as $X(t) = \sum_k a_k(t)\,\psi_k$, with mode amplitudes $a_k(t)$ capturing the instantaneous contribution of each harmonic.

- The eigenvalue λ_k relates to the spatial frequency and, under wave-like dynamics, the natural temporal frequency of mode k.
- The harmonic expansion provides a principled basis for understanding EEG/MEG signals and is compatible with electromagnetic field theories of brain function.

With the static geometry in place, we turn in the next section to the dynamics governing the evolution of the mode amplitudes $a_k(t)$.

3 Dynamics of Harmonic Modes

Having established the harmonic basis in which brain activity is represented, we now specify the dynamical equations governing the temporal evolution of the mode amplitudes $a_k(t)$. The goal is a system of equations that captures the essential physics of large-scale neural dynamics: inertia, dissipation, nonlinear interactions, external drive, and stochastic fluctuations.

3.1 Field-Level Dynamics

We posit that the spatially distributed neural activity $X(t) \in \mathbb{R}^N$ evolves according to a second-order dynamical equation of the form

$$\ddot{X}(t) + \Gamma \dot{X}(t) + \Omega^2 X(t) + \nabla_X V(X) = I(t) + \eta(t). \tag{13}$$

Here, Γ is a damping operator (generally a positive semi-definite matrix), Ω^2 encodes linear restoring forces, $V(X)$ is a nonlinear potential whose gradient introduces interactions beyond the linear regime, $I(t)$ represents external inputs (sensory, thalamic, or volitional), and $\eta(t)$ is a noise term capturing unmodeled fluctuations.

This second-order structure is motivated by several considerations:

1. **Neural mass models.** Classical models of cortical columns and thalamocortical circuits, such as the Jansen–Rit [27] and Liley models [28], feature second-order dynamics arising from the interplay of excitatory and inhibitory populations with distinct time constants.
2. **Wave phenomena.** Empirical observations of traveling waves and standing-wave patterns in cortical activity [29] are naturally accommodated by wave-like equations with second time derivatives.

3. **Oscillatory phenomenology.** EEG and MEG are dominated by rhythmic activity across multiple frequency bands. Second-order equations with appropriate parameters generate sustained or damped oscillations, matching this phenomenology.

The operators Γ and Ω^2 may in general be non-diagonal in the node basis, coupling the dynamics of different regions. However, we will see that projection onto the harmonic basis diagonalizes the linear part under natural assumptions, yielding tractable equations for the mode amplitudes.

3.2 Projection onto Harmonic Modes

We substitute the harmonic expansion $X(t) = \sum_{k=1}^{N} a_k(t)\,\psi_k$ into Eq. (13). Because the eigenmodes ψ_k are time-independent, the derivatives pass through:

$$\sum_k \ddot{a}_k(t)\,\psi_k + \Gamma \sum_k \dot{a}_k(t)\,\psi_k + \Omega^2 \sum_k a_k(t)\,\psi_k + \nabla_X V(X) = I(t) + \eta(t). \quad (14)$$

Projecting both sides onto ψ_j (i.e., taking the inner product with ψ_j) and using orthonormality, we obtain

$$\ddot{a}_j(t) + \sum_k (\psi_j^T \Gamma \psi_k)\dot{a}_k(t) + \sum_k (\psi_j^T \Omega^2 \psi_k) a_k(t) + \psi_j^T \nabla_X V(X) = I_j(t) + \xi_j(t), \quad (15)$$

where $I_j(t) = \psi_j^T I(t)$ and $\xi_j(t) = \psi_j^T \eta(t)$ are the projections of input and noise onto mode j.

3.2.1 Diagonal Approximation

A significant simplification arises if the damping and stiffness operators are diagonal in the harmonic basis—or equivalently, if they commute with the Laplacian L. In the simplest case, we assume

$$\Gamma = \mathrm{diag}(\gamma_1, \ldots, \gamma_N) \quad \text{and} \quad \Omega^2 = \mathrm{diag}(\omega_1^2, \ldots, \omega_N^2) \quad (16)$$

in the $\{\psi_k\}$ basis, where $\gamma_k \geq 0$ is the damping coefficient and $\omega_k > 0$ is the natural angular frequency of mode k. Under this assumption, the linear terms decouple across modes.

The nonlinear term $\nabla_X V(X)$, however, generically couples all modes. Defining the *mode-space potential* $U(a_1, \ldots, a_N) = V\big(\sum_k a_k \psi_k\big)$, we have

$$\psi_j^T \nabla_X V(X) = \frac{\partial U}{\partial a_j}(a_1, \ldots, a_N). \quad (17)$$

Collecting terms, we arrive at the *modewise dynamical equation*:

$$\boxed{\ddot{a}_k(t) + \gamma_k \dot{a}_k(t) + \omega_k^2 a_k(t) + \frac{\partial U}{\partial a_k}(a_1, \ldots, a_N) = I_k(t) + \xi_k(t).} \tag{18}$$

This is the central dynamical equation of the harmonic field model. Each mode amplitude $a_k(t)$ evolves as a damped, driven, nonlinear oscillator coupled to all other modes through the potential U.

3.3 Physical Interpretation of Parameters

3.3.1 Damping Coefficients γ_k

The damping coefficient γ_k controls how quickly mode k relaxes in the absence of sustained drive. Large γ_k corresponds to overdamped dynamics (rapid decay without oscillation), while small γ_k permits underdamped ringing. Physiologically, damping arises from membrane time constants, synaptic decay, and homeostatic feedback. Different modes may have different effective damping depending on the spatial distribution of inhibitory interneurons and other regulatory mechanisms [30].

3.3.2 Natural Frequencies ω_k

The natural frequency ω_k sets the intrinsic oscillation rate of mode k when decoupled from other modes and in the absence of nonlinearity. As discussed in Section 2, a natural choice is $\omega_k = \Omega_0 \sqrt{\lambda_k}$, where Ω_0 is a global frequency scale and λ_k is the Laplacian eigenvalue. This links structural (spatial) and temporal (oscillatory) properties: low-eigenvalue modes oscillate slowly, high-eigenvalue modes oscillate rapidly.

Alternatively, ω_k can be fit empirically to match observed spectral peaks, or derived from more detailed biophysical models. The key requirement is that the set $\{\omega_k\}$ spans the physiological range of brain rhythms, from delta ($\sim$1–4 Hz) to gamma ($\sim$30–100 Hz) and beyond.

3.3.3 Coupling Potential U

The potential $U(a_1, \ldots, a_N)$ encodes nonlinear interactions among modes. In the simplest case, $U = 0$ and the modes evolve independently—a linear superposition of damped oscillators. More realistically, U includes terms such as:

- **Self-interaction:** $U \supset \sum_k \frac{\mu_k}{4} a_k^4$, which saturates the growth of individual modes and prevents divergence.

- **Pairwise coupling:** $U \supset \sum_{j<k} \nu_{jk} a_j^2 a_k^2$, representing cross-frequency interactions such as phase-amplitude coupling observed in EEG [31].
- **Higher-order terms:** More complex polynomial or non-polynomial forms can capture resonance conditions, bifurcations, and other nonlinear phenomena.

The structure of U determines the repertoire of dynamical states accessible to the system—fixed points, limit cycles, quasiperiodic orbits, and chaos. In the context of consciousness, U shapes the landscape of attractor states and transitions between them, a theme we return to in Section 4.

Importantly, the coupling potential U provides a natural implementation of the dynamic gating mechanisms described in recent mixed-selectivity research [17]. The pairwise and higher-order coupling terms determine which modes interact and under what phase conditions, effectively specifying the "gating rules" that govern which variable combinations can be read out. When certain mode pairs have strong coupling (ν_{jk} large), their joint activation produces mixed representations; when coupling is weak or phase-misaligned, the modes remain functionally segregated. In this way, U implements mixed selectivity in a continuous, network-wide harmonic basis, with the nonlinear structure emerging from the geometry of inter-mode interactions rather than from the tuning properties of individual neurons.

3.3.4 Input and Noise

The term $I_k(t)$ represents deterministic input to mode k, arising from sensory afferents, thalamic relay nuclei, or top-down modulation. In a closed-eyes resting state, $I_k(t)$ may be approximately constant or slowly varying; during active perception or task performance, it carries stimulus-specific structure.

The noise term $\xi_k(t)$ models fluctuations from sources not explicitly represented in the model: synaptic noise, channel stochasticity, and unmodeled interactions with other brain regions. We typically assume $\xi_k(t)$ is Gaussian white noise with

$$\langle \xi_k(t) \rangle = 0, \quad \langle \xi_k(t) \xi_j(t') \rangle = \sigma_k^2 \delta_{kj} \delta(t - t'), \tag{19}$$

though correlated or colored noise can be incorporated if warranted by data.

3.4 Stochastic Approximation: The Ornstein–Uhlenbeck Process

For analytic tractability and connection to statistical physics, it is useful to consider a linearized, stochastic version of the mode dynamics. Neglecting the nonlinear potential ($U = 0$) and the deterministic input ($I_k = 0$), and converting the second-order equation to a first-order system, we obtain

$$\frac{d}{dt}\begin{pmatrix} a_k \\ \dot{a}_k \end{pmatrix} = \begin{pmatrix} 0 & 1 \\ -\omega_k^2 & -\gamma_k \end{pmatrix}\begin{pmatrix} a_k \\ \dot{a}_k \end{pmatrix} + \begin{pmatrix} 0 \\ \xi_k(t) \end{pmatrix}. \tag{20}$$

Stacking all modes into a vector $\mathbf{a}(t) = (a_1, \dot{a}_1, \ldots, a_N, \dot{a}_N)^T$, the system takes the form of a multivariate Ornstein–Uhlenbeck (OU) process:

$$d\mathbf{a}(t) = -A\mathbf{a}(t)\,dt + \Sigma^{1/2} dW_t, \tag{21}$$

where A is a $2N \times 2N$ drift matrix encoding damping and restoring forces, Σ is the noise covariance matrix, and W_t is a standard Wiener process.

The OU process has well-known stationary statistics. If all eigenvalues of A have positive real parts (i.e., the system is stable), the stationary covariance $C_\infty = \lim_{t\to\infty}\langle \mathbf{a}(t)\mathbf{a}(t)^T\rangle$ satisfies the Lyapunov equation

$$AC_\infty + C_\infty A^T = \Sigma. \tag{22}$$

The power spectral density of each mode can be computed analytically, yielding Lorentzian peaks centered at frequencies ω_k with widths controlled by γ_k. This provides a principled link between the harmonic model and empirical spectral analysis of EEG/MEG data.

3.5 Relationship to EEG/MEG Frequency Bands

A key insight of the harmonic field model is that the classical EEG frequency bands—delta (1–4 Hz), theta (4–8 Hz), alpha (8–13 Hz), beta (13–30 Hz), gamma (30–100 Hz)—are not fundamental dynamical entities but emergent spectral signatures of the mode amplitude dynamics. This is not merely a reinterpretation; it follows necessarily from the structure of the model. Once activity is represented in the harmonic basis, frequency bands become derived quantities—summaries of power across modes with similar natural frequencies—rather than primary objects of analysis.

Each mode k contributes power at frequencies near $\omega_k/(2\pi)$, broadened by damping γ_k and modulated by nonlinear coupling. The observed EEG spectrum is the superposition of contributions from all N modes, weighted

by their amplitudes and filtered by the measurement lead field. Different brain states (wakefulness, sleep stages, anesthesia, task engagement) correspond to different distributions of mode amplitudes $\{a_k(t)\}$, which manifest as different spectral profiles.

This perspective has several implications:

1. **Delta is not a frequency.** Delta power arises from the excitation of low-index, low-frequency modes. High delta power does not imply the brain is "oscillating at delta frequency" in a monolithic sense; it means the global, spatially smooth modes are strongly activated.

2. **Cross-frequency coupling is mode coupling.** Phenomena such as theta-gamma coupling [31] reflect interactions among modes with different natural frequencies, mediated by the nonlinear potential U.

3. **Spectral changes reflect mode redistribution.** The shift from delta-dominated sleep to alpha-dominated wakefulness corresponds to a redistribution of energy across the mode spectrum, not a change in the modes themselves.

This reframing is essential for understanding the delta paradox—how delta-rich states can support conscious experience—which we address in Section 5.

3.6 Oscillatory Gating as Mode-Level Routing

Recent work on mixed selectivity and dynamic population coding has emphasized that oscillations serve not merely as carriers of information, but as gating variables that determine which latent variables propagate forward in the brain's computational graph [17]. Within the harmonic field model, this gating mechanism acquires a precise mathematical form.

Consider the mode amplitudes in polar representation: $a_k(t) = r_k(t)e^{i\theta_k(t)}$, where the magnitude $r_k(t)$ encodes the energy in mode k and the phase $\theta_k(t)$ encodes timing. The gating interpretation proceeds as follows:

- **Spatial carriers.** Each eigenmode ψ_k defines a structured spatial pattern that serves as a carrier for variable combinations. Low-index modes span global, community-level patterns; high-index modes encode fine-grained spatial distinctions.

- **Phase-dependent propagation.** The phase $\theta_k(t)$ determines whether mode k contributes constructively or destructively to downstream circuits at any given instant. When multiple modes are phase-aligned,

their contributions sum and can influence readout; when out of phase, they cancel or remain segregated.

- **Nonlinear mixing rules.** The coupling potential $U(a_1, \ldots, a_N)$ specifies which modes interact and under what conditions. The pairwise terms $\nu_{jk} a_j^2 a_k^2$ and higher-order couplings implement the "mixing rules"—determining which mode combinations can produce conjunctive, high-dimensional representations characteristic of mixed selectivity.

This framework provides a rigorous mathematical expression of the oscillatory gating mechanism proposed in recent syntheses of population coding research [17, 14]. In traditional accounts, gating is described at the level of single neurons or local circuits; here, it emerges as a global, network-wide phenomenon operating on the harmonic basis. The advantage is that gating rules inherit the anatomical structure of the connectome: the eigenmodes ψ_k are shaped by white-matter geometry, and so the gating operations respect the brain's physical constraints.

From this perspective, oscillatory gating and harmonic field dynamics are two descriptions of the same underlying process. The question "which variables are currently being processed?" becomes "which modes are active and phase-aligned?" The rich phenomenology of cross-frequency coupling, phase-amplitude modulation, and state-dependent information routing can all be understood as manifestations of the mode-level gating structure encoded in the dynamics (18). Fig. 2 illustrates these relationships schematically.

3.7 Stability, Criticality, and the Edge of Chaos

The stability of the linearized system (21) depends on the eigenvalues of the drift matrix A. If all eigenvalues have strictly positive real parts, small perturbations decay exponentially and the system settles to a stable fixed point (modulo noise-driven fluctuations). As parameters change, eigenvalues may approach zero or the imaginary axis, signaling a bifurcation.

Near such bifurcations—often termed the "edge of chaos" or critical regime—the system exhibits enhanced sensitivity, long-range correlations, and power-law statistics [32, 33]. Empirical evidence suggests that the healthy brain operates near criticality, balancing stability and flexibility [34].

We formalize this intuition via a *criticality index* $\kappa(t)$, defined in terms

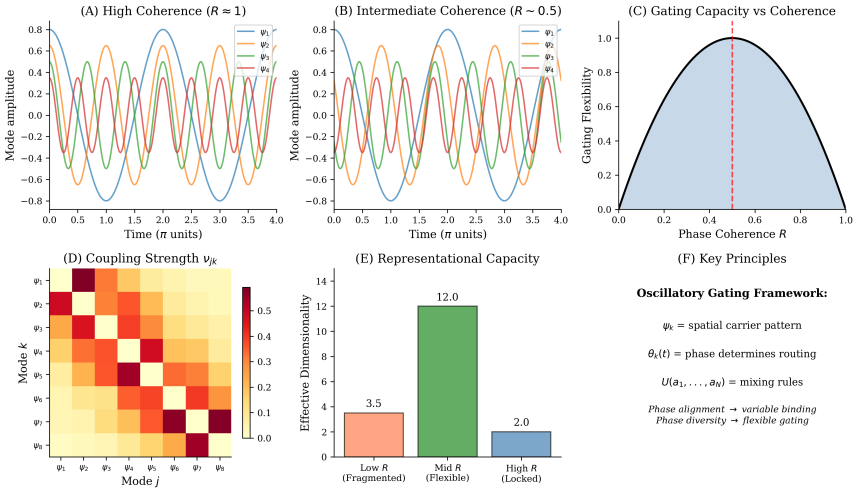

Figure 2: Oscillatory gating as mode-level routing. (A–B) Mode oscillations under high vs. intermediate phase coherence R. (C) Gating flexibility peaks at intermediate coherence. (D) Coupling matrix ν_{jk} specifies mode interaction strengths. (E) Effective representational dimensionality is highest when gating is flexible (intermediate R). (F) Summary of the oscillatory gating framework: spatial patterns ψ_k, phase-dependent routing $\theta_k(t)$, and nonlinear mixing rules U together implement the dynamic gating described in mixed-selectivity research [17].

of the leading eigenvalue $\lambda_{\max}$ of A:

$$\kappa(t) = 1 - \frac{|\Re(\lambda_{\max})|}{\lambda_{\text{crit}}}, \tag{23}$$

where λ_{crit} is a reference scale such that $\kappa \approx 1$ when the system is near criticality and $\kappa \ll 1$ when it is far from criticality (deeply stable or unstable). This index will enter our consciousness functional in Section 4.

3.8 Summary

In this section we have derived the dynamical equations for the harmonic mode amplitudes:

- The field-level dynamics (13), projected onto the harmonic basis, yield the modewise equation (18): a system of coupled, damped, driven nonlinear oscillators.

- Key parameters are the damping coefficients γ_k, natural frequencies ω_k, and nonlinear coupling potential U.
- The linearized, stochastic approximation is a multivariate Ornstein–Uhlenbeck process, amenable to analytic treatment.
- Classical EEG frequency bands are emergent from the superposition of mode contributions, not fundamental categories.
- Oscillatory gating—the dynamic routing of information through phase-dependent mode coordination—is naturally implemented by the coupling potential U and the phase structure of the mode amplitudes.
- Proximity to criticality, quantified by the index $\kappa(t)$, captures the system's dynamical regime.

With the dynamics in hand, we are now prepared to define a functional that quantifies consciousness in terms of the statistical and dynamical properties of the mode amplitudes.

4 A Consciousness Functional Based on Harmonic Field Dynamics

We now introduce the central construct of this paper: a scalar functional $C(t)$ that quantifies the degree of consciousness supported by a given harmonic field configuration. This functional is designed to capture key features associated with conscious states—complexity, integration, coherence, dynamical vitality, and proximity to criticality—while remaining grounded in the mathematically precise framework of the preceding sections.

4.1 Motivation and Desiderata

Before specifying the functional, we articulate the properties it should possess:

1. **Sensitivity to mode distribution.** Consciousness should depend not on the total power in the system but on how that power is distributed across modes. A state dominated by a single mode should have lower $C(t)$ than a state with energy spread across many modes.

2. **Integration and differentiation.** Following integrated information theory [35, 36] and related frameworks, conscious states should exhibit both differentiation (many distinguishable configurations) and integration (global coherence). Our functional should capture both aspects.

3. **Dynamical non-equilibrium.** Conscious brains are metabolically active, dissipative systems far from thermodynamic equilibrium [37]. The functional should reflect this through a measure of entropy production.

4. **Criticality.** Empirical evidence links consciousness to near-critical dynamics [34, 38]. The functional should reward states near the edge of chaos.

5. **Frequency-band agnosticism.** The functional should not privilege any particular frequency band. Delta, alpha, and gamma are all valid contributors depending on the overall configuration.

With these desiderata in mind, we construct $C(t)$ as a weighted sum of five components: mode entropy, participation ratio, phase coherence, entropy production rate, and criticality index. Within this framework, conscious experience corresponds not to activity in any particular region or frequency band, but to a global configuration of the harmonic field—an integrated pattern of interactions among spatial modes that collectively support differentiated yet unified dynamics. The substrate carries the signal, but the configuration carries the consciousness.

4.2 Mode Power and Distribution

The instantaneous power in mode k is

$$P_k(t) = |a_k(t)|^2, \tag{24}$$

where $a_k(t)$ is the (possibly complex) mode amplitude. The total power is $P_{\text{tot}}(t) = \sum_{k=1}^{N} P_k(t)$. We define the normalized mode distribution:

$$p_k(t) = \frac{P_k(t)}{\sum_{j=1}^{N} P_j(t)}, \tag{25}$$

satisfying $\sum_k p_k(t) = 1$ and $p_k(t) \geq 0$. This distribution encodes how energy is partitioned across the harmonic spectrum at time t.

4.3 Mode Entropy

The first component of the consciousness functional is the *mode entropy*:

$$H_{\text{mode}}(t) = -\sum_{k=1}^{N} p_k(t) \log p_k(t), \tag{26}$$

with the convention that $0 \log 0 = 0$. This is the Shannon entropy of the mode distribution, measuring the diversity or spread of energy across modes.

Mode entropy ranges from $H_{\text{mode}} = 0$ (all power in a single mode) to $H_{\max} = \log N$ (uniform distribution). High mode entropy indicates that the field configuration is differentiated—no single mode dominates—while low entropy indicates concentration.

Empirically, increased mode entropy has been associated with richer conscious states. Psychedelics, for instance, increase the entropy of neural activity [38], while anesthesia and deep sleep reduce it [39].

4.4 Participation Ratio

A complementary measure of mode spread is the *participation ratio*:

$$\text{PR}(t) = \frac{1}{\sum_{k=1}^{N} p_k(t)^2}. \tag{27}$$

This quantity estimates the effective number of modes with significant power. If all power is in one mode, PR = 1; if power is uniformly distributed, PR = N.

While mode entropy and participation ratio are related, they weight the tails of the distribution differently. The participation ratio is less sensitive to small probabilities and provides a robust count of "active" modes. Both are included in $C(t)$ to capture different aspects of mode diversity.

4.5 Phase Coherence

The mode amplitudes can be written in polar form: $a_k(t) = r_k(t) e^{i\theta_k(t)}$, where $r_k(t) \geq 0$ is the magnitude and $\theta_k(t) \in [0, 2\pi)$ is the phase. The phases encode the timing relationships among modes—whether they oscillate in synchrony or with independent phases.

We define a *phase coherence order parameter* analogous to the Kuramoto order parameter [40]:

$$R(t) = \left| \frac{1}{N} \sum_{k=1}^{N} e^{i\theta_k(t)} \right|. \tag{28}$$

This quantity ranges from $R = 0$ (phases uniformly distributed, no coherence) to $R = 1$ (all phases aligned, maximal coherence).

The role of phase coherence in consciousness remains debated. Some theories emphasize global synchrony as a binding mechanism [41, 5], while others highlight the importance of metastable, partially coherent states [42]. We include $R(t)$ in the functional with moderate weight, reflecting the hypothesis that consciousness involves an intermediate regime—neither complete incoherence nor rigid lock-step synchrony. This interpretation aligns with recent work on oscillatory gating in mixed-selectivity coding, which demonstrates that phase alignment determines which neuronal features combine during readout [17]. In the harmonic model, $R(t)$ captures exactly this: coherence across ψ_k determines which combinations of spatial modes can produce high-dimensional mixed representations capable of supporting flexible cognition.

The relationship between $R(t)$ and cognitive function can be understood through three regimes:

- **Low coherence ($R \approx 0$):** When mode phases are uniformly distributed, the system exhibits maximal differentiation but minimal integration. Each mode evolves independently, and no global "message" can be read out. This corresponds to fragmented or disorganized states—neurologically, perhaps seizure activity or severe delirium.

- **Intermediate coherence ($R \sim 0.3$–0.7):** Partial phase alignment enables selective binding: some mode combinations constructively interfere and reach downstream circuits, while others cancel. This metastable regime supports the flexible, context-dependent gating characteristic of wakeful cognition. Different phase configurations instantiate different "gating patterns," allowing the same harmonic spectrum to support diverse cognitive operations depending on momentary phase relationships.

- **High coherence ($R \approx 1$):** When all modes lock to the same phase, the system collapses to a single, rigid pattern. While globally integrated, such a state lacks the differentiation necessary for rich experience. This may correspond to hypersynchronous epileptiform activity or the stereotyped slow waves of deep anesthesia.

Consciousness, in this view, requires the "Goldilocks zone" of intermediate coherence—enough synchronization to bind distributed representations into unified experience, but enough phase diversity to maintain the high-dimensional, mixed-selective codes that underlie flexible thought [17, 14].

4.6 Entropy Production Rate

A defining feature of conscious systems is their non-equilibrium character. The brain consumes substantial metabolic energy to maintain organized, low-entropy states far from thermodynamic equilibrium [43]. The rate of entropy production quantifies the thermodynamic "cost" of maintaining such states.

For the linearized OU dynamics (Eq. 21), the entropy production rate can be expressed in terms of the drift matrix A, noise covariance Σ, and state covariance $C(t)$ as [44, 45]:

$$\dot{S}(t) = \mathrm{Tr}\left(A\Sigma^{-1}A^T C(t)\right) - \mathrm{Tr}(A). \tag{29}$$

At stationarity, $\dot{S} \geq 0$, with equality only at equilibrium (detailed balance). Higher $\dot{S}$ indicates the system is actively driven away from equilibrium by asymmetric dynamics.

Entropy production has been proposed as a marker of consciousness [37], with higher production associated with wakeful, engaged states and lower production with sleep or anesthesia. We include $\dot{S}(t)$ in the functional to capture this non-equilibrium signature.

4.7 Criticality Index

As discussed in Section 3, the brain appears to operate near a critical point—a phase transition between ordered and disordered regimes [32, 46]. Near criticality, the system exhibits maximal dynamic range, sensitivity, and information transmission capacity.

We quantify proximity to criticality via the index

$$\kappa(t) = 1 - \frac{|\Re(\lambda_{\max})|}{\lambda_{\mathrm{crit}}}, \tag{30}$$

where $\lambda_{\max}$ is the leading eigenvalue (most positive real part) of the linearized drift matrix A, and λ_{crit} is a reference scale. When $|\Re(\lambda_{\max})| \ll \lambda_{\mathrm{crit}}$, the system is near the stability boundary and $\kappa \approx 1$; when far from criticality, $\kappa \ll 1$ or negative.

Criticality supports the coexistence of local and global dynamics, transient synchronization, and flexible reconfiguration—properties associated with conscious processing [34].

4.8 The Combined Consciousness Functional

We now combine the five components into a single scalar measure:

$$\boxed{C(t) = \alpha \frac{H_{\text{mode}}(t)}{H_{\max}} + \beta \frac{\text{PR}(t)}{\text{PR}_{\max}} + \gamma R(t) + \delta \frac{\dot{S}(t)}{\dot{S}_{\max}} + \varepsilon \kappa(t),} \tag{31}$$

where $\alpha, \beta, \gamma, \delta, \varepsilon > 0$ are positive weights, and the normalization factors $H_{\max} = \log N$, $\text{PR}_{\max} = N$, and $\dot{S}_{\max}$ (a characteristic scale for entropy production) ensure each term is dimensionless and of order unity.

Several remarks are in order:

1. **Interpretability.** Each term has a clear interpretation: H_{mode} and PR capture differentiation, R captures integration/coherence, $\dot{S}$ captures non-equilibrium drive, and κ captures criticality.

2. **Tunability.** The weights $\alpha, \beta, \gamma, \delta, \varepsilon$ are free parameters that can be adjusted based on empirical data or theoretical considerations. Different relative weights yield different predictions about which states are more or less conscious.

3. **Non-uniqueness.** We do not claim that Eq. (31) is the unique or correct consciousness functional. Rather, it is a principled, interpretable proposal consistent with leading theories. Alternative functionals are possible and may be compared empirically.

4. **Time dependence.** The functional is evaluated at each instant t, yielding a time series $C(t)$ that tracks fluctuations in consciousness. Averaging over time gives a mean level; variance reflects stability.

4.9 Relationship to Existing Measures

The consciousness functional $C(t)$ relates to several existing complexity and consciousness measures:

- **Lempel-Ziv complexity and perturbational complexity index (PCI).** These measures quantify the compressibility or response diversity of neural signals [39]. High mode entropy and participation ratio correspond to low compressibility and high PCI.

- **Integrated information (Φ).** Tononi's integrated information theory defines consciousness as the irreducible information generated by

a system [35]. While $C(t)$ does not compute Φ directly, the combination of entropy (differentiation) and coherence (integration) captures related intuitions.

- **Global workspace measures.** Global workspace theory emphasizes the broadcasting of information across distant brain regions [47]. Low-index, globally coherent modes in our framework correspond to workspace activity; high $R(t)$ may index broadcasting.
- **Criticality measures.** Neuronal avalanche analyses and power-law exponents have been used to assess criticality [32]. The index $\kappa(t)$ provides a complementary, eigenvalue-based measure.

Thus, $C(t)$ synthesizes insights from multiple theoretical traditions into a unified, computationally tractable functional.

4.10 Computation and Estimation

In practice, $C(t)$ is computed as follows:

1. **Obtain mode amplitudes.** Given neural activity data $X(t)$ (e.g., source-reconstructed EEG), project onto the harmonic basis: $a_k(t) = \psi_k^T X(t)$.
2. **Compute power distribution.** Calculate $P_k(t) = |a_k(t)|^2$ and normalize to obtain $p_k(t)$.
3. **Evaluate mode entropy and participation ratio.** Apply the definitions above.
4. **Extract phases.** Use the Hilbert transform or analytic signal representation to obtain $\theta_k(t)$, then compute $R(t)$.
5. **Estimate entropy production.** This requires knowledge of the drift matrix A and noise covariance Σ, which can be estimated from data via system identification or assumed from model parameters.
6. **Compute criticality index.** Evaluate the eigenvalues of A and apply the definition of $\kappa(t)$.
7. **Combine terms.** Weight and sum to obtain $C(t)$.

Windowed or time-averaged versions of these quantities can be used to smooth fluctuations and yield more stable estimates.

4.11 Predictions and Testable Hypotheses

The consciousness functional generates several predictions:

1. **Wakefulness vs. deep sleep.** Wakeful states should have higher $C(t)$ than deep NREM sleep, driven by higher mode entropy, participation ratio, and entropy production.

2. **Anesthesia.** General anesthesia should reduce $C(t)$ by decreasing entropy production and shifting dynamics away from criticality.

3. **Psychedelics.** Psychedelic states, associated with increased neural entropy [38], should show elevated mode entropy and possibly $C(t)$.

4. **Dreaming.** REM sleep and dreaming should have intermediate $C(t)$—lower than wakefulness but higher than deep NREM—due to preserved mode diversity and criticality.

5. **Delta-rich consciousness.** Crucially, states with high delta power need not have low $C(t)$ if mode entropy, coherence, and criticality remain high. This is the delta paradox, to which we now turn.

4.12 Summary

In this section we have defined a consciousness functional $C(t)$ that integrates five components:

- **Mode entropy** $H_{\text{mode}}(t)$: diversity of power distribution.
- **Participation ratio** $\text{PR}(t)$: effective number of active modes.
- **Phase coherence** $R(t)$: synchronization among modes.
- **Entropy production rate** $\dot{S}(t)$: non-equilibrium drive.
- **Criticality index** $\kappa(t)$: proximity to the edge of chaos.

The functional is mathematically explicit, computationally tractable, and connects to existing theories of consciousness. Its key virtue is that it depends on the *configuration* of the harmonic field—the distribution, coherence, and dynamics of mode amplitudes—rather than on any single frequency band or regional activation. Fig. 3 illustrates how the five components and the combined $C(t)$ vary across brain states. This sets the stage for resolving the delta paradox.

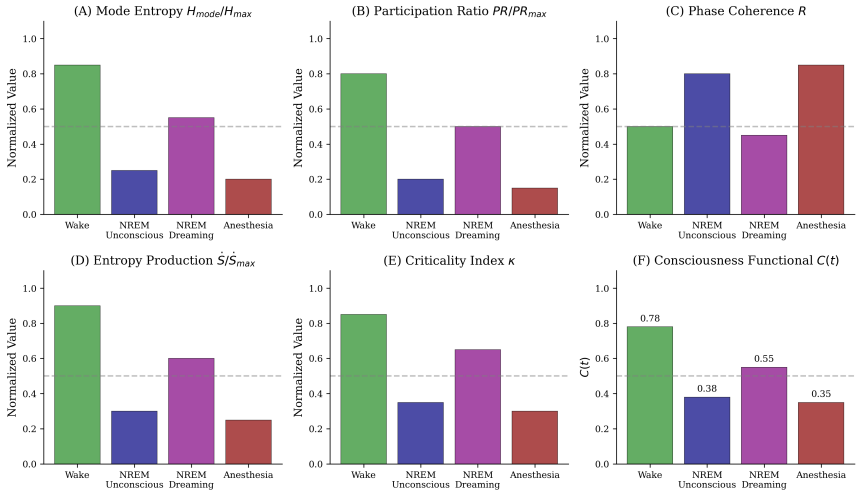

Figure 3: Components of the consciousness functional $C(t)$ across four brain states: wake, NREM unconscious, NREM dreaming, and anesthesia. (A–E) Each panel shows one normalized component: mode entropy H_{mode}, participation ratio PR, phase coherence R, entropy production $\dot{S}$, and criticality index κ. (F) The combined consciousness functional. Wake exhibits the highest $C(t)$; NREM unconscious and anesthesia the lowest; NREM dreaming shows intermediate values despite substantial low-mode power. The phase coherence component R reflects phase-dependent mode-gating as described in mixed-selectivity research [17].

5 Resolving the Delta Paradox

One of the most persistent puzzles in consciousness research is the relationship between slow-wave (delta) activity and conscious experience. The conventional view holds that delta oscillations (1–4 Hz) are a signature of unconsciousness: they dominate deep non-REM (NREM) sleep, increase under anesthesia, and are associated with reduced responsiveness. Yet a growing body of evidence challenges this simple association. Dreams can occur during NREM sleep despite prominent delta waves; certain meditative states feature enhanced slow oscillations alongside vivid awareness; and pathological conditions sometimes dissociate delta power from behavioral responsiveness. We term this the *delta paradox*: the observation that high delta power is neither necessary nor sufficient for unconsciousness. Recent analyses of sleep and dream phenomenology increasingly support the view

that delta-rich neural states can be compatible with conscious experience under specific conditions, provided that global integration is maintained [15].

In this section, we demonstrate how the harmonic field model resolves the delta paradox by showing that consciousness is a property of the *overall field configuration*—the distribution, coherence, and dynamics of mode amplitudes—not of any single frequency band.

5.1 The Traditional Interpretation

The association between delta activity and unconsciousness dates to the earliest days of EEG [48]. Subsequent research established a robust empirical correlation:

- **Sleep staging.** Sleep is conventionally staged by EEG criteria, with deep NREM (stages N2 and N3) characterized by increasing delta power [49]. Arousals from deep sleep are difficult, and dream reports are sparse.
- **Anesthesia.** General anesthetics such as propofol and sevoflurane increase delta power while suppressing consciousness [50].
- **Pathology.** Coma and vegetative states often exhibit diffuse delta slowing [51].

These observations led to the widespread assumption that delta activity *causes* or *reflects* unconsciousness. In its strongest form, the claim is that delta oscillations are intrinsically incompatible with conscious experience.

5.2 Challenges to the Traditional View

Several lines of evidence challenge this interpretation:

1. **NREM dreaming.** Dream reports can be elicited from NREM sleep, including stages with substantial delta power [8]. These reports, while often less vivid than REM dreams, indicate preserved subjective experience.
2. **Lucid dreaming in NREM.** Rare but documented cases of lucid dreaming during NREM sleep [52] demonstrate that high-level metacognition can coexist with slow-wave activity.

3. **Meditation.** Advanced meditators in certain traditions report maintaining awareness during states resembling deep sleep, sometimes with increased delta power [9].

4. **Anesthesia awareness.** Patients occasionally report conscious experience during anesthesia despite EEG patterns suggesting deep sedation [10].

5. **Dissociation in disorders.** Some patients with disorders of consciousness show behavioral unresponsiveness despite EEG complexity measures suggesting preserved cortical differentiation [39].

These observations suggest that delta power is an imperfect marker of consciousness. Something more than the presence or absence of a particular frequency band must determine whether experience is present. Fig. 4 illustrates how mode power distributions differ across conscious and unconscious states.

5.3 Delta Waves as Low-Index Mode Activation

The harmonic field model provides a principled explanation. Recall that neural activity is expanded as

$$X(t) = \sum_{k=1}^{N} a_k(t)\, \psi_k, \tag{32}$$

where the mode index k is ordered by Laplacian eigenvalue λ_k. Low-index modes (small λ_k) are spatially smooth, engaging large swathes of cortex in coordinated activity. High-index modes are spatially complex, reflecting finer-grained patterns.

The natural frequency of mode k scales with $\sqrt{\lambda_k}$:

$$\omega_k \propto \sqrt{\lambda_k}. \tag{33}$$

Thus, low-index modes oscillate slowly (delta/theta range), while high-index modes oscillate rapidly (beta/gamma range).

Delta power in the EEG is therefore a signature of strong activation of low-index, spatially global modes. It does not indicate that the brain is "oscillating at delta frequency" in a homogeneous sense; rather, it indicates that the first few harmonic modes—the "bass notes" of the connectome—are energized.

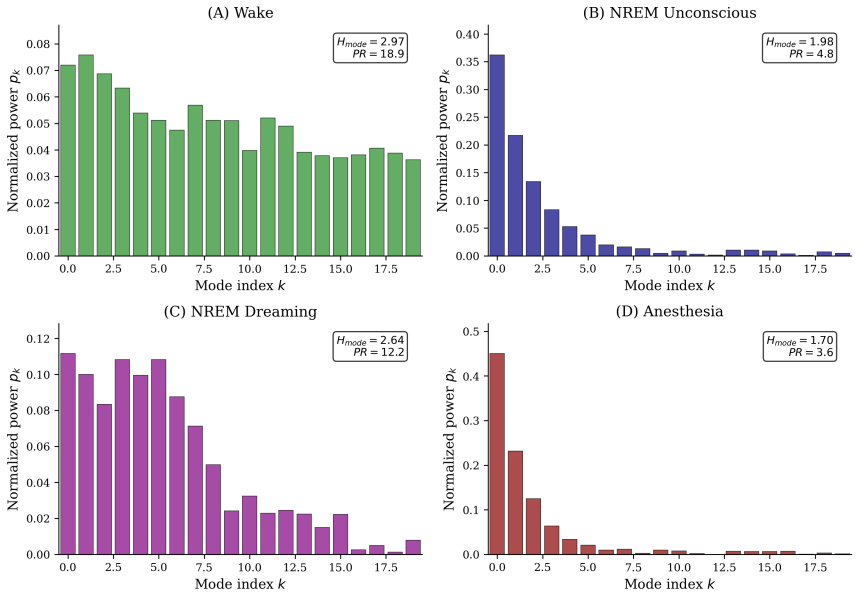

Figure 4: Synthetic mode power distributions p_k for four brain states. (A) Wake: broad distribution with high entropy. (B) NREM unconscious: concentrated in low-index modes. (C) NREM dreaming: low-mode power present but broader distribution. (D) Anesthesia: strongly concentrated in lowest modes. Mode entropy H_{mode} and participation ratio PR are displayed for each state, showing that wake and NREM dreaming maintain higher diversity than unconscious states. In the mixed-selectivity framework, these distributions reflect phase-dependent mode-gating: states with broader distributions support more flexible, high-dimensional representations [17].

5.4 Why Delta Power Alone Does Not Determine Consciousness

The consciousness functional $C(t)$ depends on five quantities: mode entropy H_{mode}, participation ratio PR, phase coherence R, entropy production $\dot{S}$, and criticality index κ. Crucially, none of these is determined by the power in any single mode or frequency band.

Consider a state with high delta power, meaning $P_1(t), P_2(t), \ldots, P_m(t)$ are large for the first m low-frequency modes. Two scenarios are possible:

5.4.1 Scenario A: Delta Dominance with Low $C(t)$

If most power is concentrated in just one or two low-index modes while higher modes are suppressed, the mode distribution $\{p_k\}$ will be sharply peaked. In this case:

- H_{mode} is low (concentrated distribution).
- PR is low (few effective modes).
- R may be high (trivial coherence among few active modes) or low (depending on phase structure).
- $\dot{S}$ may be low if the system is near equilibrium.
- κ may be low if the system is far from criticality (deeply stable or pathological).

The resulting $C(t)$ is low, corresponding to reduced consciousness. This is the typical deep NREM or anesthesia scenario: delta dominance with impoverished mode diversity.

5.4.2 Scenario B: Delta Presence with High $C(t)$

If low-index modes are active but so are many mid- and high-index modes, the distribution $\{p_k\}$ may be broad despite substantial delta power. In this case:

- H_{mode} is moderate to high (broad distribution).
- PR is moderate to high (many effective modes).
- R reflects nontrivial phase relationships across modes.
- $\dot{S}$ may be substantial if the system is driven away from equilibrium.
- κ may be near unity if the system is close to criticality.

The resulting $C(t)$ can be moderate to high, indicating preserved consciousness despite delta activity. This corresponds to NREM dreaming, meditative awareness, or other delta-rich conscious states.

5.5 Mathematical Illustration

To make this concrete, consider a simplified two-regime model:

Regime 1: Deep NREM (unconscious). Let $p_1 = 0.8$, $p_2 = 0.15$, and spread the remaining 0.05 across modes $k = 3, \ldots, N$. Then:

$$H_{\text{mode}} \approx -0.8 \log 0.8 - 0.15 \log 0.15 - 0.05 \log(0.05/(N-2)) \approx 0.6 \text{ (low)}, \tag{34}$$

$$\text{PR} \approx 1/(0.8^2 + 0.15^2 + \cdots) \approx 1.5 \text{ (low)}. \tag{35}$$

Suppose also $R = 0.9$ (high coherence among the dominant modes), $\dot{S}/\dot{S}_{\max} = 0.2$ (low drive), and $\kappa = 0.3$ (far from criticality). Then

$$C(t) \approx \alpha \cdot 0.1 + \beta \cdot 0.015 + \gamma \cdot 0.9 + \delta \cdot 0.2 + \varepsilon \cdot 0.3, \tag{36}$$

which, for typical weights, yields a low value.

Regime 2: NREM with dreaming (conscious). Let $p_1 = 0.3$, $p_2 = 0.2$, and spread 0.5 more broadly across modes $k = 3, \ldots, 20$. Then:

$$H_{\text{mode}} \approx 2.5 \text{ (moderate, higher diversity)}, \tag{37}$$

$$\text{PR} \approx 5 \text{ (more effective modes)}. \tag{38}$$

Suppose $R = 0.5$ (partial coherence), $\dot{S}/\dot{S}_{\max} = 0.5$ (moderate drive), and $\kappa = 0.7$ (nearer criticality). Then

$$C(t) \approx \alpha \cdot 0.4 + \beta \cdot 0.05 + \gamma \cdot 0.5 + \delta \cdot 0.5 + \varepsilon \cdot 0.7, \tag{39}$$

yielding a substantially higher value—despite both states having significant delta (mode 1) power. Fig. 5 illustrates this comparison schematically.

5.6 Case Analyses

We now apply the framework to specific empirical scenarios.

5.6.1 Deep NREM Sleep Without Dream Reports

Subjects awakened from deep NREM often report no conscious experience [8]. The harmonic model explains this as a state of extreme mode concentration: power is funneled into a handful of low-index modes, mode entropy and participation ratio collapse, the system is far from criticality, and entropy production is minimal. The consciousness functional $C(t)$ is correspondingly low.

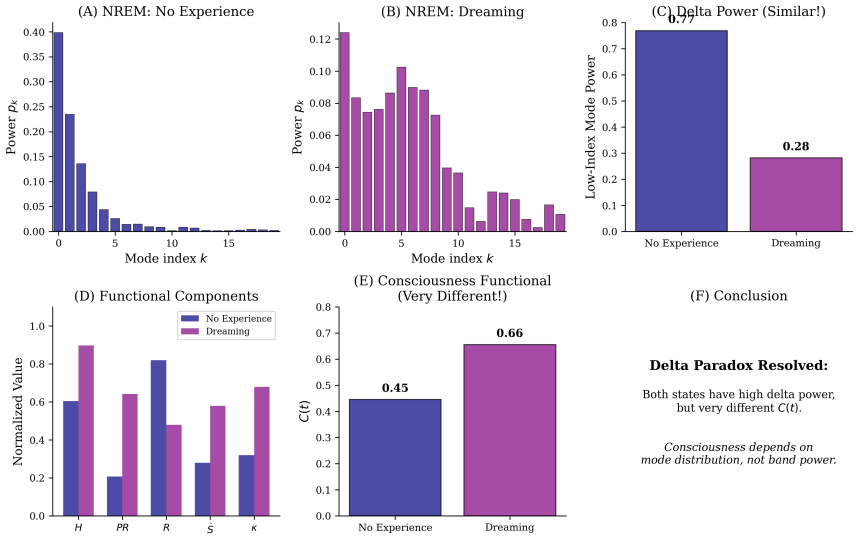

Figure 5: The delta paradox resolved. (A–B) Mode power distributions for NREM without experience and NREM with dreaming. (C) Both states exhibit similar low-index mode power ("delta"). (D) Comparison of consciousness functional components shows that despite similar delta power, the dreaming state has higher mode entropy, participation ratio, entropy production, and criticality. (E) The consciousness functional $C(t)$ differs dramatically between states. (F) Conclusion: consciousness depends on mode distribution and dynamics, not band power alone. The difference between states reflects distinct phase-dependent gating configurations, with the dreaming state supporting richer mixed-selectivity representations [17].

5.6.2 NREM Sleep With Dream Reports

A subset of NREM awakenings yield dream reports, sometimes detailed ones [8]. The model predicts that these epochs have broader mode distributions—while delta modes remain active, mid-frequency modes are also engaged, maintaining diversity. Phase coherence is intermediate, criticality is preserved, and $C(t)$ is elevated relative to dreamless NREM.

5.6.3 REM Sleep

REM sleep features reduced delta power and increased faster activity. In mode terms, power shifts toward higher-index modes. Mode entropy and participation ratio increase, phase coherence becomes more complex, and

$C(t)$ rises. The vivid, narrative character of REM dreams corresponds to rich harmonic configurations.

5.6.4 General Anesthesia

Anesthetics like propofol enhance delta/alpha oscillations while suppressing high-frequency activity [50]. In harmonic terms, anesthesia concentrates power in low-index modes, reduces entropy production, and pushes the system away from criticality. The result is a collapsed $C(t)$, consistent with loss of consciousness.

5.6.5 Wakefulness

Wakeful states exhibit broad-spectrum activity with power distributed across many modes. Mode entropy is high, participation ratio is large, entropy production is maximal, and the system hovers near criticality. $C(t)$ is at its highest during alert, engaged wakefulness.

5.6.6 Meditative States

Some meditation traditions cultivate awareness alongside slow-wave activity [9]. The model suggests these states achieve high $C(t)$ not by suppressing delta but by maintaining diversity and criticality: low-index modes are active, but so are others, and the overall configuration remains complex and far from equilibrium.

5.7 Frequencies as Spectral Signatures, Not Causes

The central lesson of the harmonic field model is that *frequency bands are spectral signatures of the field state, not causes of consciousness or its absence*. Delta, theta, alpha, beta, and gamma are labels for regions of the power spectrum; they summarize which modes are active but do not determine the functional properties of the field.

Consciousness emerges from the *configuration* of the harmonic field:

- How is power distributed across modes (entropy, participation)?
- How are phases coordinated (coherence)?
- How far is the system from equilibrium (entropy production)?
- How close is the system to criticality?

Two states with identical delta power can have vastly different $C(t)$ depending on the answers to these questions. Conversely, two states with similar $C(t)$ can have very different spectral profiles.

5.8 Mixed-Selectivity Constraints Dissolve the Delta Ambiguity

The resolution of the delta paradox gains additional mechanistic clarity when viewed through the lens of mixed selectivity and oscillatory gating [17]. In this framework, consciousness requires not merely the presence of diverse mode activity, but the capacity for flexible, context-dependent combination of latent variables—precisely what mixed-selective neural codes provide.

The key insight is that delta-dominated states fail to support consciousness not because delta oscillations are intrinsically incompatible with awareness, but because the mode configurations typical of unconscious delta states lack the phase structure necessary for high-dimensional mixed representations:

1. **Gating collapse.** In deep NREM sleep and anesthesia, the phase relationships among modes become stereotyped. When $R(t) \to 1$, all modes lock to the same phase, eliminating the possibility of selective gating. Without phase diversity, the system cannot dynamically reconfigure which mode combinations reach downstream circuits—the computational flexibility underlying cognition is lost.

2. **Reduced mixing dimensionality.** Mixed selectivity depends on nonlinear combinations of input variables. In the harmonic model, this requires activation of multiple modes with coupling through U. When power concentrates in only one or two low-index modes, the nonlinear interaction terms $\nu_{jk} a_j^2 a_k^2$ become negligible, and the effective dimensionality of the representation collapses.

3. **Loss of phase-dependent routing.** Oscillatory gating operates by selectively aligning or misaligning mode phases to control information flow. In unconscious delta states, this routing mechanism fails: either phases are locked (no routing flexibility) or phases are completely dissociated from downstream readout (no coherent signal).

Conversely, delta-rich conscious states—such as NREM dreaming or certain meditative states—preserve the gating machinery despite substantial low-frequency power:

- Multiple modes remain active, even if low-index modes dominate in absolute power.
- Phase coherence $R(t)$ stays in the intermediate regime, permitting selective binding.
- The coupling structure U continues to support nonlinear mixing among the active modes.
- Entropy production $\dot{S}$ remains elevated, indicating active, non-equilibrium dynamics.

This analysis reveals that the delta paradox is, at root, a paradox about gating capacity rather than frequency content. The question is not "how much delta power is present?" but "can the system still perform flexible, phase-dependent mode routing?" When the answer is yes, consciousness can persist regardless of spectral profile; when no, consciousness fades regardless of which frequencies dominate.

5.9 Implications for Clinical and Research Practice

The resolution of the delta paradox has practical implications:

1. **Anesthesia monitoring.** Depth-of-anesthesia monitors based on spectral power or suppression ratios may miss states where delta power is high but consciousness is preserved. Monitors incorporating mode entropy, criticality, or related measures may be more sensitive.
2. **Disorders of consciousness.** Patients in vegetative or minimally conscious states should be assessed not just for delta slowing but for the complexity and diversity of their harmonic configurations. A patient with high delta but preserved mode entropy may have more residual awareness than one with uniform slow activity.
3. **Sleep and dream research.** Predicting dream reports from EEG should incorporate harmonic measures beyond band power. Epochs with high delta but maintained mode diversity are more likely to yield reports.
4. **Neurofeedback and meditation.** Training protocols that target "alpha enhancement" or "delta suppression" may be misguided if they ignore the overall harmonic configuration. What matters is the shape of the mode distribution, not the power in any single band.

5.10 Summary

The delta paradox—the coexistence of strong delta activity with conscious experience—is resolved by recognizing that consciousness depends on the global configuration of the harmonic field, not on any single frequency band:

- Delta waves reflect activation of low-index, spatially global modes.
- The consciousness functional $C(t)$ depends on mode entropy, participation ratio, coherence, entropy production, and criticality—none of which is determined by delta power alone.
- States with high delta can have high or low $C(t)$ depending on the distribution of power across all modes.
- Frequency bands are emergent spectral signatures, not fundamental determinants of conscious content.
- The mixed-selectivity framework clarifies that what distinguishes conscious from unconscious delta states is the preservation of flexible, phase-dependent gating capacity.

This perspective dissolves the apparent paradox and provides a more nuanced, configuration-based understanding of the relationship between neural oscillations and consciousness. Under this formulation, conscious experience corresponds to the global field achieving a dynamically rich yet integrated configuration, in which multiple spatial modes interact coherently without collapsing into uniformity or fragmenting into disorganized activity. This resolution emphasizes the central principle of the harmonic model: consciousness is determined by the richness, integration, and dynamical structure of the global harmonic field, not by power in any specific frequency band.

6 Compatibility with Geometric Field Theories

The harmonic field model developed in the preceding sections provides a self-contained, empirically grounded framework for understanding consciousness in terms of brain dynamics. However, the formalism is deliberately general: the graph Laplacian and its eigenmodes are mathematical tools that can be applied to any weighted network, and the dynamical equations are agnostic about the ultimate physical substrate. This generality opens the door to deeper theoretical extensions—embeddings of the brain-level model into

broader geometric or field-theoretic frameworks that may illuminate the physical basis of consciousness.

In this section, we discuss the compatibility of our approach with such extensions. We emphasize that the model as presented makes no commitment to any specific underlying geometry; rather, it is designed to interface smoothly with a wide class of geometric field theories. Our aim is to position the harmonic field model as a bridge between neuroscientific data and more fundamental physical descriptions, without prejudging which (if any) such description is correct.

6.1 The Graph Laplacian as a Discrete Approximation

The graph Laplacian $L = D - A$ introduced in Section 2 is a discrete operator defined on the nodes of the structural connectome. Its eigenmodes ψ_k are vectors in $\mathbb{R}^N$, where N is the number of parcellation regions.

This discrete structure can be viewed as a finite approximation to a continuous spatial domain. On a smooth manifold $\mathcal{M}$ equipped with a Riemannian metric, the natural generalization of the graph Laplacian is the *Laplace–Beltrami operator* Δ_g, defined in terms of the metric tensor g:

$$\Delta_g f = \frac{1}{\sqrt{|g|}} \partial_i \left(\sqrt{|g|} g^{ij} \partial_j f \right). \tag{40}$$

The eigenfunctions of Δ_g are the continuous analogues of the graph Laplacian eigenmodes. On a sphere, they are the spherical harmonics; on more complex geometries, they reflect the curvature and topology of the manifold.

The brain's white-matter connectivity defines an effective geometry in which proximity is measured by connection strength rather than Euclidean distance. The graph Laplacian eigenmodes are thus "connectome harmonics"—harmonics defined with respect to this connectivity-induced geometry [11]. In the continuum limit (e.g., as the parcellation becomes finer), the graph Laplacian converges to a Laplace–Beltrami operator on an effective manifold whose metric encodes the structural connectome [53].

6.2 Possible Extensions to Curved and Higher-Dimensional Geometries

If the brain's effective geometry is not simply a discrete graph but rather a discretization of some underlying continuous manifold, then the harmonic field model inherits structure from that manifold. Several possibilities merit consideration:

6.2.1 Cortical Surface Geometry

The cerebral cortex is a folded two-dimensional sheet embedded in three-dimensional space. Laplacian eigenmodes computed on the cortical surface mesh capture patterns of cortical organization [54]. These surface harmonics may provide a more anatomically faithful basis than parcellation-based graph harmonics, particularly for high-resolution data.

6.2.2 Curved Manifolds with Non-Euclidean Metrics

More speculatively, the effective geometry of brain connectivity may be curved in ways not captured by the cortical surface alone. If the connectome is better described by a manifold with non-trivial curvature—positive, negative, or varying across regions—then the harmonic eigenmodes will reflect this curvature. Negatively curved (hyperbolic) spaces, for instance, have different spectral properties than flat or positively curved spaces, including different density-of-states distributions at low frequencies.

6.2.3 Higher-Dimensional Spaces

Some theoretical frameworks posit that brain dynamics unfold in higher-dimensional state spaces, with the observed three-dimensional structure being a projection or section. In such scenarios, the relevant Laplacian would be defined on this higher-dimensional space, and the brain-level harmonics would be restrictions of higher-dimensional eigenfunctions.

6.3 Field Theories on Manifolds

The dynamical equation for the mode amplitudes,

$$\ddot{a}_k(t) + \gamma_k \dot{a}_k(t) + \omega_k^2 a_k(t) + \frac{\partial U}{\partial a_k} = I_k(t) + \xi_k(t), \tag{41}$$

is formally identical to a field equation expanded in a spectral basis. On a continuous manifold, the analogous equation would govern the amplitude of each eigenfunction of the Laplace–Beltrami operator.

This structure is familiar from field theories in physics:

- **Scalar field theory.** A scalar field $\phi(x,t)$ on a manifold satisfies a wave equation $\partial_t^2\phi + \gamma\partial_t\phi + \Delta_g\phi + V'(\phi) = J$, where $V(\phi)$ is a potential and J is an external source. Expanding ϕ in eigenfunctions of Δ_g yields equations for the mode amplitudes of the same form as our modewise dynamics.

- **Electromagnetic fields.** The vector potential A_μ and field tensor $F_{\mu\nu}$ satisfy equations that can be spectrally decomposed on curved backgrounds, with mode amplitudes obeying oscillator equations modified by curvature.

- **Quantum fields.** In quantum field theory, field excitations are quantized oscillators for each mode. The classical limit of a quantum field on a manifold is a collection of coupled oscillators indexed by the spectrum of the Laplacian.

The harmonic field model of consciousness thus has the same mathematical form as a classical field theory on an effective geometry. This raises the intriguing possibility that brain dynamics are best understood as the low-energy, coarse-grained manifestation of a more fundamental field.

6.4 Electromagnetic Field Theories of Consciousness

A concrete example of a geometric field theory relevant to consciousness is the electromagnetic field theory of mind [26, 55]. On this view, the brain's endogenous electromagnetic field—generated by neural currents and propagating through tissue—is the physical substrate of consciousness. The EM field is a bona fide physical field obeying Maxwell's equations, and its dynamics can be expanded in spatial eigenmodes determined by the geometry and conductivity of the head.

The harmonic field model is fully compatible with this perspective. The neural activity field $X(t)$ defined in Section 2 is intimately related to the current sources of the EM field. The connectome harmonics ψ_k can be interpreted as approximate spatial modes of the EM field, with the mode amplitudes $a_k(t)$ tracking the time-varying strength of each mode.

If the EM field is indeed the substrate of consciousness, then the consciousness functional $C(t)$ proposed here is a proxy for the informational and dynamical properties of the EM field itself. Future work could refine the model by computing harmonics directly from the geometry of EM field propagation rather than from the structural connectome alone.

6.5 Criticality and Phase Transitions in Field Theories

The criticality index $\kappa(t)$ introduced in Section 4 captures proximity to a dynamical phase transition—a point where the system's qualitative behavior changes (e.g., from stable to oscillatory, or from ordered to disordered). In

the language of field theory, such transitions are associated with diverging correlation lengths, power-law fluctuations, and universal scaling behavior.

Field theories on curved manifolds can exhibit geometry-dependent phase transitions. The curvature of the underlying space modifies the effective mass of excitations, potentially tuning the system toward or away from criticality. If the brain's effective geometry has regions of varying curvature, this could create a spatially heterogeneous criticality landscape, with some regions more critical than others.

The harmonic model is agnostic about the source of criticality. Whether the brain self-organizes to criticality through homeostatic mechanisms [33], is tuned by neuromodulation [56], or inherits critical behavior from an underlying field-theoretic structure, the formalism captures the outcome via the criticality index $\kappa(t)$.

6.6 Constraints on Underlying Geometry

While the harmonic field model does not require a specific underlying geometry, empirical data can constrain the possibilities. The observed spectrum of connectome harmonics—the distribution of eigenvalues $\{\lambda_k\}$ and the spatial structure of eigenvectors $\{\psi_k\}$—carries information about the effective geometry:

- **Spectral dimension.** The rate at which eigenvalues grow with mode index encodes the effective dimensionality of the space. A d-dimensional manifold has $\lambda_k \sim k^{2/d}$ for large k (Weyl's law). Deviations from this scaling may indicate anomalous or fractal effective geometry.

- **Spectral gaps.** Gaps in the eigenvalue spectrum can indicate topological features such as disconnected components, holes, or bottlenecks.

- **Eigenfunction localization.** The spatial extent of eigenfunctions reflects the geometry of the manifold. Localized eigenfunctions suggest inhomogeneous or disordered geometry; extended eigenfunctions suggest regularity.

By analyzing the spectral properties of empirically derived connectomes, one can infer constraints on any proposed underlying geometry. A successful geometric field theory of consciousness should reproduce these spectral properties from first principles.

6.7 Toward a Unified Framework

The ultimate aspiration of this line of research is a unified framework in which:

1. The brain's structural connectome arises as the effective geometry of a more fundamental field or manifold.
2. Neural dynamics are the low-energy, coarse-grained limit of field dynamics on this geometry.
3. Consciousness corresponds to specific configurations of the field—those with high mode entropy, participation, coherence, entropy production, and criticality—as captured by the functional $C(t)$.
4. The delta paradox and other puzzles are resolved by recognizing that consciousness is a property of field configurations, not of local observables like frequency power.

Such a framework would bridge the gap between neuroscience and physics, grounding the phenomenology of consciousness in the mathematics of fields and geometry. The harmonic field model presented here is a step in that direction: it provides a rigorous, neuroscience-compatible formalism that can interface with deeper theories while remaining empirically testable at the brain level.

6.8 Epistemological Caution

We emphasize that the compatibility of our model with geometric field theories does not imply endorsement of any particular theory. The claims made in this paper are:

1. The harmonic field model is a useful and principled way to describe brain-level consciousness.
2. It resolves empirical puzzles like the delta paradox.
3. It is mathematically compatible with a broad class of underlying geometries.

Whether consciousness is ultimately explained by electromagnetic fields, quantum fields, curved manifolds, or some other structure is an open question beyond the scope of this paper. Our goal is to provide a bridge—a formal language in which such questions can be posed and, eventually, answered.

6.9 Summary

In this section we have discussed the compatibility of the harmonic field model with geometric field theories:

- The graph Laplacian can be viewed as a discrete approximation to a Laplace–Beltrami operator on an effective manifold.
- The modewise dynamics have the same form as field equations expanded in a spectral basis.
- Electromagnetic field theories of consciousness are naturally accommodated by the formalism.
- Criticality and phase transitions can be understood in field-theoretic terms.
- Spectral properties of the connectome constrain possible underlying geometries.

The harmonic field model thus serves as a bridge between empirical neuroscience and more fundamental physical descriptions, positioning consciousness research at the interface of biology, physics, and mathematics.

Although this paper employs the Laplacian of the empirical structural connectome as the generator of harmonic modes, the underlying formalism is inherently geometry-agnostic. Any substrate—biological, physical, or computational—that supports a harmonic decomposition could instantiate an analogous dynamical system. This generality ensures that the present framework is not tied to a specific anatomical representation but is compatible with any broader geometric or physical theory that admits a well-defined Laplace-type operator. Whether the relevant operator acts on neural tissue, electromagnetic field propagation, or a more fundamental manifold, the same harmonic expansion applies. The present work should therefore be seen as a bridge layer: experimentally grounded, mathematically explicit, and positioned to interface with deeper geometric theories without depending on them.

7 Discussion and Future Directions

We have presented a harmonic field model of consciousness that represents brain activity as a superposition of connectome eigenmodes, specifies dynamical equations for mode amplitudes, defines a consciousness functional

$C(t)$ combining entropy, participation, coherence, entropy production, and criticality, and applies this framework to resolve the delta paradox. In this final section, we discuss the broader implications of the model, its relationship to existing theories and measures, empirical predictions, limitations, and directions for future research. These results align closely with recent proposals emphasizing dynamic gating, multiscale integration, and high-dimensional representational structure in neural population coding [14].

A central theme emerging from this work is the deep connection between the harmonic field framework and contemporary understanding of neural population codes. The mixed-selectivity paradigm [17] has established that cognitive flexibility depends on high-dimensional neural representations in which single neurons encode nonlinear combinations of task-relevant variables, with oscillatory phase and neuromodulatory state dynamically gating which combinations are functionally active. The harmonic model provides a precise mathematical substrate for these phenomena: the eigenmodes ψ_k define the spatial patterns available for combination; the coupling potential U specifies the nonlinear mixing rules; and the phase structure $\theta_k(t)$ implements gating. This correspondence suggests that the harmonic field model is not merely a convenient decomposition but reflects the actual computational geometry through which the brain implements flexible, state-dependent cognition. The implications extend beyond consciousness research to the broader question of how structured neural dynamics support adaptive behavior.

As large-scale neuroimaging datasets and increasingly detailed structural connectomes accumulate, it is becoming evident that harmonic models provide a principled and scalable foundation for understanding global brain dynamics. Unlike traditional band-based approaches, which impose externally defined boundaries on neural activity, harmonic analyses emerge directly from the structural geometry of the system. In this sense, the move toward harmonic field models should be viewed not as an optional alternative, but as a natural and necessary next step in theoretical neuroscience.

The results presented in this work position harmonic models not as speculative alternatives but as the mathematically inevitable description of activity on a structured network. Once the brain is recognized as a spatially extended field constrained by a fixed connectivity operator, a harmonic basis is not optional: it is the unique eigen-decomposition of that operator. Any field-based account of brain dynamics must reduce to the same structure.

7.1 Summary of Contributions

The main contributions of this paper are:

1. **A principled mathematical framework.** We have provided a rigorous formalism for describing large-scale brain dynamics in terms of graph Laplacian eigenmodes, second-order coupled oscillator dynamics, and a composite consciousness functional.

2. **Resolution of the delta paradox.** By showing that consciousness depends on the overall configuration of the harmonic field—not on power in any single frequency band—we dissolve the apparent contradiction between delta activity and conscious experience.

3. **Synthesis of theoretical traditions.** The consciousness functional $C(t)$ integrates insights from information-theoretic measures (entropy, complexity), dynamical systems theory (criticality), non-equilibrium thermodynamics (entropy production), and synchronization theory (phase coherence).

4. **A bridge to deeper theories.** The formalism is compatible with geometric field theories, positioning it as an interface between empirical neuroscience and more fundamental physical descriptions.

7.2 Relationship to Existing Complexity and Consciousness Measures

Several existing measures of neural complexity and consciousness can be situated within the harmonic framework:

7.2.1 Perturbational Complexity Index (PCI)

PCI measures the algorithmic complexity of the EEG response to transcranial magnetic stimulation [39]. High PCI indicates that the brain produces complex, differentiated responses—consistent with high mode entropy and participation ratio in the harmonic model. PCI has proven effective at distinguishing conscious from unconscious states; the harmonic functional $C(t)$ can be viewed as a model-based generalization.

7.2.2 Lempel–Ziv Complexity

Lempel–Ziv (LZ) complexity quantifies the compressibility of a time series [57]. Applied to EEG, LZ complexity is elevated in wakeful and psychedelic

states [58]. In harmonic terms, high LZ complexity corresponds to a broad, dynamic mode distribution that resists compression.

7.2.3 Integrated Information (Φ)

Integrated information theory (IIT) proposes that consciousness corresponds to integrated information, denoted Φ [35, 36]. Computing Φ exactly is intractable for large systems, but the intuition—that conscious systems are both differentiated and integrated—is captured by the combination of mode entropy (differentiation) and phase coherence (integration) in $C(t)$.

7.2.4 Global Workspace Measures

Global workspace theory emphasizes the broadcasting of information across distant brain regions [47]. In the harmonic model, global broadcasting corresponds to the activation of low-index, spatially extended modes with significant coherence. The functional $C(t)$ rewards such configurations through the coherence term $R(t)$.

7.2.5 Criticality Measures

Neuronal avalanche analyses quantify proximity to criticality via power-law exponents and branching ratios [32]. The criticality index $\kappa(t)$ provides an alternative, eigenvalue-based measure that can be computed from the linearized dynamics.

The harmonic model thus provides a unifying language in which these diverse measures can be compared, combined, and extended.

7.2.6 Mixed Selectivity and Oscillatory Gating

Recent advances in understanding mixed selectivity provide particularly strong mechanistic support for the harmonic field framework [17]. The emerging consensus that oscillatory phase and neuromodulatory context dynamically gate which variable combinations reach downstream readout circuits maps directly onto the harmonic model's architecture. Specifically, the model provides a mathematically structured substrate for mixed selectivity: global (low-index) modes correspond to broadcast variables that can be widely read out; mid- and high-index modes implement local nonlinear combinations with finer spatial structure; and the coherence structure among modes specifies the gating rules that determine which combinations are functionally active. This correspondence suggests that the harmonic basis is not

merely a convenient decomposition but reflects the actual computational geometry through which the brain implements flexible, high-dimensional representations. Future work should test whether the gating variables described in mixed-selectivity research correspond directly to mode-phase-dependent readout, and whether manipulating phase relationships among specific harmonic modes alters the effective dimensionality of neural population codes.

7.3 Empirical Tests and Predictions

The model generates several empirically testable predictions:

7.3.1 Sleep Staging

The functional $C(t)$ should track sleep stages, with highest values in wakefulness, intermediate values in REM and light NREM, and lowest values in deep NREM. Critically, within NREM, epochs with dream reports should have higher $C(t)$ than epochs without, despite similar delta power.

7.3.2 Anesthesia

During induction of general anesthesia, $C(t)$ should decline before loss of responsiveness and recover during emergence. The model predicts that monitoring $C(t)$ (or its components) will outperform simple spectral measures for detecting awareness.

7.3.3 Psychedelics

Psychedelic states should show elevated mode entropy and $C(t)$, consistent with the "entropic brain" hypothesis [38]. The model further predicts that the increase in $C(t)$ will be correlated with subjective intensity and altered-state phenomenology.

7.3.4 Disorders of Consciousness

Patients in vegetative or minimally conscious states should be classifiable by $C(t)$. Those with higher $C(t)$—due to preserved mode entropy, coherence, or criticality—may have better prognosis or show signs of covert awareness.

7.3.5 Meditation

Advanced meditators in states of "objectless awareness" should maintain moderate-to-high $C(t)$ despite altered spectral profiles, including enhanced

slow-wave activity. The model predicts that the key factor is preserved mode diversity and criticality, not suppression of any particular band.

7.3.6 Cross-Species Comparisons

By computing connectome harmonics and $C(t)$ for non-human animals with available connectome data (e.g., macaques, mice), the model can generate predictions about comparative consciousness. Species with richer harmonic spectra and more critical dynamics should exhibit more complex behavior.

7.3.7 Summary of Distinguishing Predictions

Beyond the domain-specific predictions above, the harmonic framework yields several general predictions that distinguish it from conventional band-centric approaches:

- Dream-rich NREM sleep should exhibit high mode entropy and moderate entropy production despite strong delta power.
- General anesthesia should produce a characteristic reduction in mid-level eigenmode interaction rather than a uniform suppression across frequencies.
- Psychedelic states should show increased participation ratio and enhanced coupling among intermediate eigenmodes, reflecting an expanded harmonic workspace.
- Meditative states with sustained awareness may combine elevated low-frequency power with preserved or enhanced mid-frequency mode coherence.
- Transitions into unconsciousness should be marked by a collapse of multi-mode interaction structure rather than by any specific change in a single band.
- Cross-state discrimination: the functional $C(t)$ should reliably distinguish conscious from unconscious states across diverse conditions (sleep, anesthesia, pathology) better than single-band power measures.
- Differentiating high-delta conscious vs. high-delta unconscious states: epochs with similar delta power but different dream reports should differ systematically in mode entropy and criticality.

- Computational validation: simulated networks with Laplacian dynamics should exhibit predictable relationships between connectivity structure, harmonic spectrum, and emergent $C(t)$.
- Machine consciousness criteria: if the harmonic framework captures essential features of consciousness, artificial systems with analogous connectivity operators and harmonic dynamics should exhibit similar functional signatures when $C(t)$ is computed from their activity.

These predictions distinguish the harmonic field model from conventional band-centric interpretations and can be evaluated directly using source-reconstructed EEG, MEG, or high-density fMRI.

This also clarifies why a harmonic description is substrate-agnostic: any sufficiently complex information-bearing medium with a stable connectivity operator—biological, artificial, or hybrid—will admit a harmonic spectrum. If consciousness corresponds to field configuration rather than biological specifics, similar functional signatures could emerge in any architecture that supports rich, integrated harmonic dynamics.

7.4 Limitations and Open Problems

The harmonic field model has several limitations that should be acknowledged:

7.4.1 Dependence on Parcellation

The graph Laplacian and its eigenmodes depend on the choice of brain parcellation. Different atlases yield different harmonics, and there is no universally agreed-upon parcellation. Future work should explore robustness across parcellations and the use of continuous surface-based harmonics.

7.4.2 Tractography Limitations

Structural connectivity estimated from diffusion MRI is subject to noise, crossing fibers, and limitations in resolving short-range connections. The accuracy of the harmonic basis depends on the quality of the tractography. Improvements in diffusion imaging and reconstruction algorithms will benefit the model.

7.4.3 Model Simplifications

The dynamical model assumes second-order dynamics with diagonal damping and stiffness in the harmonic basis. Real neural dynamics may violate these assumptions. The nonlinear potential U is left unspecified; empirical or biophysical constraints are needed to determine its form.

7.4.4 Weight Selection

The weights $\alpha, \beta, \gamma, \delta, \varepsilon$ in the consciousness functional are free parameters. Their values affect predictions and must be calibrated against empirical data. Alternatively, machine learning methods could be used to learn weights that optimize discrimination between conscious and unconscious states.

7.4.5 Phenomenology Mapping

The functional $C(t)$ quantifies a scalar "level" of consciousness but does not address the content or quality of experience. The "hard problem" of how physical processes give rise to subjective experience remains untouched. Future extensions might incorporate phenomenological distinctions by analyzing the specific pattern of mode activations, not just their aggregate statistics.

7.4.6 Temporal Resolution

The model describes instantaneous configurations of the harmonic field. Consciousness, however, may depend on temporal structure—sequences, transitions, and dynamics over time. Extending the functional to incorporate temporal complexity (e.g., entropy rates, predictive information) is a natural direction.

7.5 Future Directions

Several avenues for future research are suggested by this work:

7.5.1 Empirical Validation

The most pressing need is systematic empirical validation. This requires:

- High-quality connectome data and parcellations.

- EEG/MEG/fMRI data from subjects in varied states of consciousness (wake, sleep, anesthesia, psychedelics, meditation, disorders of consciousness).
- Computation of harmonic decomposition and $C(t)$ from these data.
- Correlation of $C(t)$ with behavioral reports, task performance, and clinical assessments.

7.5.2 Biophysical Refinement

The dynamical model can be refined by incorporating biophysically realistic parameters:

- Natural frequencies ω_k derived from membrane time constants and conduction delays.
- Damping coefficients γ_k reflecting inhibitory-excitatory balance.
- Nonlinear potentials U capturing synaptic saturation and homeostatic plasticity.

7.5.3 Real-Time Monitoring

A practical goal is real-time computation of $C(t)$ from streaming EEG. This could enable:

- Improved anesthesia monitoring.
- Neurofeedback for meditation or cognitive enhancement.
- Brain-computer interfaces guided by consciousness state.

7.5.4 Integration with Other Theories

The harmonic model should be integrated with and compared to other formal theories of consciousness:

- Integrated information theory: Can Φ be approximated or bounded using harmonic methods?
- Global workspace theory: Do low-index, coherent modes correspond to workspace activity?
- Predictive processing: Can the free energy principle be formulated in harmonic terms?

7.5.5 Extension to Subcortical and Cerebellar Structures

The current model focuses on cortical connectivity. Extending the framework to include thalamus, basal ganglia, brainstem, and cerebellum would provide a more complete picture. These structures play crucial roles in arousal, gating, and coordination that likely affect $C(t)$.

7.5.6 Developmental and Evolutionary Perspectives

How does the harmonic structure of the brain change during development, aging, and across species? Longitudinal and comparative studies could reveal how the capacity for consciousness emerges and degrades.

7.6 Concluding Remarks

The harmonic field model offers a mathematically rigorous, empirically testable, and theoretically integrative approach to consciousness. By shifting focus from frequency bands to field configurations—from "how much delta?" to "how is power distributed, coherent, and dynamically organized?"—it provides a more nuanced understanding of the relationship between brain activity and conscious experience. This shift is not merely preferable but necessary: once the brain is recognized as a structured network, the harmonic basis is mathematically determined, and the question of consciousness becomes a question about field configuration.

The resolution of the delta paradox illustrates the power of this approach: what appeared to be a contradiction dissolves once we recognize that delta waves are simply a signature of low-index mode activation, and consciousness depends on the overall harmonic configuration. The same logic applies more broadly: no single neural observable—frequency, region, neurotransmitter—determines consciousness. What matters is the global pattern.

Whether the harmonic field model is ultimately subsumed into a deeper geometric or physical theory remains to be seen. For now, it provides a productive framework for organizing empirical findings, generating predictions, and connecting neuroscience to the broader scientific understanding of complex systems. We hope it will contribute to the ongoing effort to understand how the brain generates the most remarkable phenomenon in the known universe: conscious experience.

A Mathematical Details

This appendix provides detailed derivations and technical elaborations of the mathematical framework presented in the main text. We include derivations of the mode dynamics from the field equation, the linearization yielding the Ornstein–Uhlenbeck process, formal expressions for entropy production, and alternative formulations of the coherence and criticality indices.

A.1 Derivation of Mode Dynamics from the Field Equation

We begin with the field-level dynamical equation (Eq. 13 in the main text):

$$\ddot{X}(t) + \Gamma \dot{X}(t) + \Omega^2 X(t) + \nabla_X V(X) = I(t) + \eta(t), \tag{42}$$

where $X(t) \in \mathbb{R}^N$ is the neural activity vector, Γ and Ω^2 are $N \times N$ matrices representing damping and restoring forces, $V(X)$ is a nonlinear potential, $I(t)$ is external input, and $\eta(t)$ is noise.

A.1.1 Expansion in Eigenmodes

Substitute the harmonic expansion $X(t) = \sum_{k=1}^{N} a_k(t)\psi_k$, where ψ_k are the orthonormal eigenvectors of the graph Laplacian L with eigenvalues λ_k. Since the ψ_k are time-independent:

$$\dot{X}(t) = \sum_k \dot{a}_k(t)\psi_k, \quad \ddot{X}(t) = \sum_k \ddot{a}_k(t)\psi_k. \tag{43}$$

Substituting into the field equation:

$$\sum_k \ddot{a}_k\psi_k + \Gamma \sum_k \dot{a}_k\psi_k + \Omega^2 \sum_k a_k\psi_k + \nabla_X V = I + \eta. \tag{44}$$

A.1.2 Projection onto Mode j

Taking the inner product with ψ_j and using orthonormality ($\psi_j^T\psi_k = \delta_{jk}$):

$$\ddot{a}_j + \sum_k (\psi_j^T \Gamma \psi_k)\dot{a}_k + \sum_k (\psi_j^T \Omega^2 \psi_k)a_k + \psi_j^T \nabla_X V = \psi_j^T I + \psi_j^T \eta. \tag{45}$$

A.1.3 Diagonal Assumption

If Γ and Ω^2 are diagonal in the $\{\psi_k\}$ basis (i.e., they commute with L), then:

$$\psi_j^T \Gamma \psi_k = \gamma_j \delta_{jk}, \quad \psi_j^T \Omega^2 \psi_k = \omega_j^2 \delta_{jk}. \tag{46}$$

This yields the simplified equation:

$$\ddot{a}_j + \gamma_j \dot{a}_j + \omega_j^2 a_j + \psi_j^T \nabla_X V = I_j + \xi_j, \tag{47}$$

where $I_j = \psi_j^T I$ and $\xi_j = \psi_j^T \eta$.

A.1.4 Mode-Space Potential

Define the mode-space potential $U(a_1, \ldots, a_N) = V\left(\sum_k a_k \psi_k\right)$. By the chain rule:

$$\frac{\partial U}{\partial a_j} = \sum_i \frac{\partial V}{\partial X_i} \frac{\partial X_i}{\partial a_j} = \sum_i \frac{\partial V}{\partial X_i} (\psi_j)_i = \psi_j^T \nabla_X V. \tag{48}$$

Thus, we obtain the final modewise equation:

$$\boxed{\ddot{a}_k(t) + \gamma_k \dot{a}_k(t) + \omega_k^2 a_k(t) + \frac{\partial U}{\partial a_k} = I_k(t) + \xi_k(t).} \tag{49}$$

A.2 Linearization and the Ornstein–Uhlenbeck Process

For analytic tractability, we linearize the mode dynamics by neglecting the nonlinear potential ($U = 0$) and deterministic input ($I_k = 0$).

A.2.1 State-Space Formulation

Define the state vector for mode k as $\mathbf{z}_k = (a_k, \dot{a}_k)^T$. The linearized second-order equation becomes a first-order system:

$$\frac{d\mathbf{z}_k}{dt} = \begin{pmatrix} 0 & 1 \\ -\omega_k^2 & -\gamma_k \end{pmatrix} \mathbf{z}_k + \begin{pmatrix} 0 \\ \xi_k(t) \end{pmatrix}. \tag{50}$$

Let $A_k = \begin{pmatrix} 0 & -1 \\ \omega_k^2 & \gamma_k \end{pmatrix}$ (note the sign convention for the drift matrix). Then:

$$\frac{d\mathbf{z}_k}{dt} = -A_k \mathbf{z}_k + \mathbf{b}_k \xi_k(t), \tag{51}$$

where $\mathbf{b}_k = (0, 1)^T$.

A.2.2 Full System

Stacking all modes into a $2N$-dimensional vector $\mathbf{z} = (\mathbf{z}_1, \ldots, \mathbf{z}_N)^T$:

$$d\mathbf{z}(t) = -A\mathbf{z}(t)\,dt + B\,d\mathbf{W}_t, \tag{52}$$

where $A = \mathrm{diag}(A_1, \ldots, A_N)$ is a block-diagonal $2N \times 2N$ matrix, B encodes the noise injection, and $\mathbf{W}_t$ is a standard N-dimensional Wiener process.

If the noise has covariance $\langle \xi_k(t)\xi_j(t')\rangle = \sigma_k^2 \delta_{kj}\delta(t-t')$, then the noise covariance matrix is $\Sigma = B\,\mathrm{diag}(\sigma_1^2, \ldots, \sigma_N^2)\,B^T$.

This is a multivariate Ornstein–Uhlenbeck (OU) process:

$$d\mathbf{z}(t) = -A\mathbf{z}(t)\,dt + \Sigma^{1/2} d\mathbf{W}_t. \tag{53}$$

A.2.3 Stationary Distribution

If all eigenvalues of A have positive real parts (stable system), the process has a Gaussian stationary distribution with mean zero and covariance C_∞ satisfying the Lyapunov equation:

$$AC_\infty + C_\infty A^T = \Sigma. \tag{54}$$

For the block-diagonal structure, this decouples into N independent 2×2 Lyapunov equations, one per mode.

A.2.4 Power Spectral Density

The power spectral density (PSD) of mode k is:

$$S_k(\omega) = \frac{\sigma_k^2}{(\omega_k^2 - \omega^2)^2 + (\gamma_k \omega)^2}. \tag{55}$$

This is a Lorentzian centered at $\omega \approx \omega_k$ (for underdamped modes with $\gamma_k < 2\omega_k$), with width proportional to γ_k. The total power in mode k is:

$$\langle a_k^2 \rangle = \int_{-\infty}^{\infty} \frac{S_k(\omega)}{2\pi} d\omega = \frac{\sigma_k^2}{2\gamma_k \omega_k^2}. \tag{56}$$

A.3 Entropy Production Rate

A.3.1 General Formula

For a multivariate OU process $d\mathbf{z} = -A\mathbf{z}\,dt + \Sigma^{1/2} d\mathbf{W}_t$, the entropy production rate in the stationary state is [44, 45]:

$$\dot{S} = \mathrm{Tr}\left((A - A^T)\Sigma^{-1} C_\infty\right), \tag{57}$$

where C_∞ is the stationary covariance.

An equivalent expression is:

$$\dot{S} = \mathrm{Tr}\left(A\Sigma^{-1}A^T C_\infty\right) - \mathrm{Tr}(A). \tag{58}$$

A.3.2 Interpretation

Entropy production measures the irreversibility of the dynamics—the rate at which the system produces entropy in its environment. For equilibrium systems (satisfying detailed balance), $\dot{S} = 0$. For driven, non-equilibrium systems, $\dot{S} > 0$.

In the context of brain dynamics, high entropy production indicates that the system is actively maintained away from equilibrium by metabolic processes. This is associated with wakeful, conscious states.

A.3.3 Estimation from Data

Given time-series data, A and Σ can be estimated via maximum likelihood or moment matching. The covariance C_∞ can be estimated directly from the data. These estimates allow computation of $\dot{S}$.

A.4 Alternative Formulations of Phase Coherence

A.4.1 Kuramoto Order Parameter

The phase coherence $R(t)$ defined in the main text is the magnitude of the Kuramoto order parameter:

$$R(t)e^{i\Phi(t)} = \frac{1}{N}\sum_{k=1}^{N} e^{i\theta_k(t)}, \tag{59}$$

where $\Phi(t)$ is the mean phase. $R \in [0, 1]$ measures the degree of phase synchronization.

A.4.2 Weighted Coherence

A weighted version accounts for differences in mode power:

$$R_w(t) = \left|\frac{\sum_k P_k(t)e^{i\theta_k(t)}}{\sum_k P_k(t)}\right| = \left|\sum_k p_k(t)e^{i\theta_k(t)}\right|. \tag{60}$$

This gives more weight to high-power modes.

A.4.3 Pairwise Phase Locking

An alternative measure is the mean pairwise phase-locking value (PLV):

$$\mathrm{PLV}(t) = \frac{2}{N(N-1)} \sum_{j<k} \left| \langle e^{i(\theta_j(t) - \theta_k(t))} \rangle_T \right|, \tag{61}$$

where $\langle \cdot \rangle_T$ denotes a time average over a window. This captures the consistency of phase relationships.

A.4.4 Metastability

The variance of $R(t)$ over time measures metastability [42]:

$$\chi = \mathrm{Var}_t[R(t)]. \tag{62}$$

High metastability indicates the system fluctuates between coherent and incoherent states—a signature of flexible, adaptive dynamics.

A.5 Alternative Formulations of the Criticality Index

A.5.1 Eigenvalue-Based Index

The criticality index $\kappa(t)$ in the main text is defined as:

$$\kappa(t) = 1 - \frac{|\Re(\lambda_{\max})|}{\lambda_{\mathrm{crit}}}, \tag{63}$$

where $\lambda_{\max}$ is the eigenvalue of A with the largest (least negative) real part. Near a bifurcation, $\Re(\lambda_{\max}) \to 0$, so $\kappa \to 1$.

A.5.2 Branching Ratio

In the theory of neuronal avalanches, criticality is characterized by the branching ratio σ—the average number of downstream activations per activation [32]. At criticality, $\sigma = 1$; subcritical systems have $\sigma < 1$; supercritical systems have $\sigma > 1$. The branching ratio can be estimated from spike data and used as an alternative criticality index.

A.5.3 Power-Law Exponents

Critical systems exhibit power-law distributions of avalanche sizes and durations:

$$P(s) \propto s^{-\tau}, \quad P(d) \propto d^{-\alpha}, \tag{64}$$

with exponents $\tau \approx 1.5$ and $\alpha \approx 2$ for mean-field criticality. Deviations from these exponents indicate distance from criticality. A criticality index can be constructed from the deviation:

$$\kappa_{\text{exponent}} = 1 - \frac{|\tau - 1.5|}{0.5}. \tag{65}$$

A.5.4 Susceptibility

The susceptibility χ measures the system's response to perturbations. Near criticality, susceptibility diverges. A normalized susceptibility can serve as a criticality index:

$$\kappa_\chi = \frac{\chi}{\chi_{\max}}, \tag{66}$$

where $\chi_{\max}$ is a reference maximum.

A.6 Properties of the Mode Entropy

A.6.1 Bounds

The mode entropy $H_{\text{mode}} = -\sum_k p_k \log p_k$ satisfies:

$$0 \leq H_{\text{mode}} \leq \log N, \tag{67}$$

with the lower bound achieved when all power is in one mode ($p_j = 1$ for some j, $p_k = 0$ otherwise) and the upper bound achieved for the uniform distribution ($p_k = 1/N$ for all k).

A.6.2 Relationship to Participation Ratio

The participation ratio $\text{PR} = 1/\sum_k p_k^2$ satisfies:

$$1 \leq \text{PR} \leq N. \tag{68}$$

For a distribution with m equally weighted modes ($p_k = 1/m$ for $k = 1, \ldots, m$), $\text{PR} = m$ and $H_{\text{mode}} = \log m$. Thus:

$$H_{\text{mode}} = \log(\text{PR}) \tag{69}$$

for such distributions. More generally, for arbitrary distributions:

$$\log(\text{PR}) \leq H_{\text{mode}} \leq \log N, \tag{70}$$

with equality on the left for flat-topped distributions.

A.6.3 Sensitivity to Tails

Mode entropy is more sensitive to small probabilities than the participation ratio. If many modes have small but nonzero power, H_{mode} increases significantly, while PR may remain modest. This justifies including both in the consciousness functional.

A.7 Normalization of the Consciousness Functional

The consciousness functional is:

$$C(t) = \alpha \frac{H_{\text{mode}}}{H_{\max}} + \beta \frac{\text{PR}}{\text{PR}_{\max}} + \gamma R + \delta \frac{\dot{S}}{\dot{S}_{\max}} + \varepsilon \kappa. \tag{71}$$

Each term is normalized to $[0, 1]$:

- $H_{\text{mode}}/H_{\max} \in [0, 1]$ with $H_{\max} = \log N$.
- $\text{PR}/\text{PR}_{\max} \in [0, 1]$ with $\text{PR}_{\max} = N$.
- $R \in [0, 1]$ by definition.
- $\dot{S}/\dot{S}_{\max} \in [0, 1]$ where $\dot{S}_{\max}$ is an empirically determined or theoretically motivated upper bound.
- $\kappa \in (-\infty, 1]$, but in practice is bounded; if needed, κ can be clipped to $[0, 1]$.

With positive weights $\alpha + \beta + \gamma + \delta + \varepsilon = 1$, the functional $C(t)$ lies in $[0, 1]$, facilitating interpretation as a normalized consciousness level.

A.8 Stability Analysis of Mode Dynamics

A.8.1 Linear Stability

For the linearized single-mode equation $\ddot{a}_k + \gamma_k \dot{a}_k + \omega_k^2 a_k = 0$, the characteristic equation is:

$$s^2 + \gamma_k s + \omega_k^2 = 0, \tag{72}$$

with roots:

$$s_\pm = \frac{-\gamma_k \pm \sqrt{\gamma_k^2 - 4\omega_k^2}}{2}. \tag{73}$$

- **Underdamped** ($\gamma_k < 2\omega_k$): Complex conjugate roots with negative real parts. Oscillatory decay.

- **Critically damped** ($\gamma_k = 2\omega_k$): Repeated real root. Fastest non-oscillatory decay.
- **Overdamped** ($\gamma_k > 2\omega_k$): Two distinct negative real roots. Exponential decay without oscillation.

For all $\gamma_k > 0$ and $\omega_k > 0$, the equilibrium $a_k = 0$ is stable.

A.8.2 Bifurcations

As parameters vary, the system may undergo bifurcations:

- **Hopf bifurcation**: If $\gamma_k \to 0$, eigenvalues approach the imaginary axis, and a limit cycle may emerge.
- **Saddle-node bifurcation**: Changes in the nonlinear potential U can create or destroy fixed points.
- **Pitchfork bifurcation**: Symmetry-breaking transitions in U can split stable equilibria.

The criticality index κ tracks proximity to such bifurcations.

A.9 Summary of Key Equations

For reference, we collect the key equations of the harmonic field model:

1. **Graph Laplacian:** $L = D - A$, with eigenproblem $L\psi_k = \lambda_k \psi_k$.
2. **Harmonic expansion:** $X(t) = \sum_{k=1}^{N} a_k(t)\psi_k$.
3. **Mode dynamics:** $\ddot{a}_k + \gamma_k \dot{a}_k + \omega_k^2 a_k + \frac{\partial U}{\partial a_k} = I_k + \xi_k$.
4. **Mode power:** $P_k(t) = |a_k(t)|^2$, normalized distribution $p_k = P_k / \sum_j P_j$.
5. **Mode entropy:** $H_{\text{mode}} = -\sum_k p_k \log p_k$.
6. **Participation ratio:** $\text{PR} = 1/\sum_k p_k^2$.
7. **Phase coherence:** $R = \left|\frac{1}{N}\sum_k e^{i\theta_k}\right|$.
8. **Entropy production:** $\dot{S} = \text{Tr}(A\Sigma^{-1}A^T C) - \text{Tr}(A)$.
9. **Criticality index:** $\kappa = 1 - |\Re(\lambda_{\max})|/\lambda_{\text{crit}}$.

10. **Consciousness functional:** $C(t) = \alpha \frac{H_{\text{mode}}}{H_{\max}} + \beta \frac{\text{PR}}{\text{PR}_{\max}} + \gamma R + \delta \frac{\dot{S}}{\dot{S}_{\max}} + \varepsilon\kappa$.

These equations form the mathematical core of the harmonic field model of consciousness.

Acknowledgements

The author thanks the open neuroscience community for ongoing discussions on mixed selectivity, oscillatory gating, and large-scale structure–function coupling, which contributed to the conceptual clarity of this work.

References

[1] Christof Koch, Marcello Massimini, Melanie Boly, and Giulio Tononi. Neural correlates of consciousness: progress and problems. *Nature Reviews Neuroscience*, 17(5):307–321, 2016.

[2] Stanislas Dehaene and Jean-Pierre Changeux. Experimental and theoretical approaches to conscious processing. *Neuron*, 70(2):200–227, 2011.

[3] György Buzsáki. *Rhythms of the Brain*. Oxford University Press, New York, 2006.

[4] Wolfgang Klimesch. EEG alpha and theta oscillations reflect cognitive and memory performance: a review and analysis. *Brain Research Reviews*, 29(2-3):169–195, 1999.

[5] Pascal Fries. Rhythms for cognition: communication through coherence. *Neuron*, 88(1):220–235, 2015.

[6] Mircea Steriade. Grouping of brain rhythms in corticothalamic systems. *Neuroscience*, 137(4):1087–1106, 2006.

[7] Jaan Aru, Talis Bachmann, Wolf Singer, and Lucia Melloni. Distilling the neural correlates of consciousness. *Neuroscience & Biobehavioral Reviews*, 36(2):737–746, 2012.

[8] Francesca Siclari, Benjamin Baird, Lampros Perogamvros, Giulio Bernardi, Joshua J LaRocque, Brady Riedner, Melanie Boly, Bradley R Postle, and Giulio Tononi. The neural correlates of dreaming. *Nature Neuroscience*, 20(6):872–878, 2017.

[9] Fabio Ferrarelli, Richard Smith, Daniela Dentico, Brady A Riedner, Corinna Zennig, Ruth M Benca, Antoine Lutz, Richard J Davidson, and Giulio Tononi. Experienced mindfulness meditators exhibit higher parietal-occipital EEG gamma activity during NREM sleep. *PLoS One*, 8(8):e73417, 2013.

[10] George A Mashour, Beverley A Orser, and Niven Bhana. Awareness during anesthesia. *Canadian Journal of Anesthesia*, 58(2):206–215, 2011.

[11] Selen Atasoy, Isaac Donnelly, and Suresh Bhattacharyya. Human brain networks function in connectome-specific harmonic waves. *Nature Communications*, 7(1):10340, 2016.

[12] Peter A Robinson, Xiao Zhao, Kevin M Aquino, John D Griffiths, Somwrita Sarkar, and Grishma Mehta-Pandejee. Eigenmodes of brain activity: Neural field theory predictions and comparison with experiment. *NeuroImage*, 142:79–98, 2016.

[13] David J Chalmers. Facing up to the problem of consciousness. *Journal of Consciousness Studies*, 2(3):200–219, 1995.

[14] Earl K Miller, Mikael Lundqvist, and Andre M Bastos. Working memory and the organization of brain computations. *Neuron*, 112(3):340–358, 2024.

[15] Giulio Tononi, Melanie Boly, and Chiara Cirelli. Sleep, dreaming, and consciousness. *Neuron*, 112(8):1199–1217, 2024.

[16] Maria Giulia Preti and Dimitri Van De Ville. Decoupling of brain function from structure reveals regional behavioral specialization in humans. *Nature Communications*, 10(1):4747, 2019.

[17] Nancy Padilla-Coreano, Selin Canber, Jyotsna Bhagat, Rachel Lauman, Rohan Bhattacharyya, and Earl K. Miller. Mixed selectivity and oscillatory gating as organizing principles for flexible population coding. *Neuron*, 112(14):2255–2270, 2024.

[18] Olaf Sporns, Giulio Tononi, and Rolf Kötter. The human connectome: a structural description of the human brain. *PLoS Computational Biology*, 1(4):e42, 2005.

[19] Patric Hagmann, Leila Cammoun, Xavier Gigandet, Reto Meuli, Christopher J Honey, Van J Wedeen, and Olaf Sporns. Mapping the structural core of human cerebral cortex. *PLoS Biology*, 6(7):e159, 2008.

[20] Timothy EJ Behrens, Mark W Woolrich, Mark Jenkinson, Heidi Johansen-Berg, Rita G Nunes, Stuart Clare, Paul M Matthews, J Michael Brady, and Stephen M Smith. Characterization and propagation of uncertainty in diffusion-weighted MR imaging. *Magnetic Resonance in Medicine*, 50(5):1077–1088, 2003.

[21] Miroslav Fiedler. Algebraic connectivity of graphs. *Czechoslovak Mathematical Journal*, 23(2):298–305, 1973.

[22] Christoph von der Malsburg. Neural mechanisms of visual grouping. *Current Opinion in Neurobiology*, 10(5):524–529, 2000.

[23] Paul L Nunez and Ramesh Srinivasan. *Electric Fields of the Brain: The Neurophysics of EEG*. Oxford University Press, New York, 2nd edition, 2006.

[24] Sylvain Baillet. Magnetoencephalography for brain electrophysiology and imaging. *Nature Neuroscience*, 20(3):327–339, 2017.

[25] Costas A Anastassiou, Rodrigo Perin, Henry Markram, and Christof Koch. Ephaptic coupling of cortical neurons. *Nature Neuroscience*, 14(2):217–223, 2011.

[26] Johnjoe McFadden. Integrating information in the brain's EM field: the cemi field theory of consciousness. *Neuroscience of Consciousness*, 2020(1):niaa016, 2020.

[27] Ben H Jansen and Vincent G Rit. Electroencephalogram and visual evoked potential generation in a mathematical model of coupled cortical columns. *Biological Cybernetics*, 73(4):357–366, 1995.

[28] David TJ Liley, Peter J Cadusch, and Mathew P Dafilis. A spatially continuous mean field theory of electrocortical activity. *Network: Computation in Neural Systems*, 13(1):67–113, 2002.

[29] Lyle Muller, Frédéric Chavane, John Reynolds, and Suresh Bhattacharyya. Cortical travelling waves: mechanisms and computational principles. *Nature Reviews Neuroscience*, 19(5):255–268, 2018.

[30] Hugh R Wilson and Jack D Cowan. Excitatory and inhibitory interactions in localized populations of model neurons. *Biophysical Journal*, 12(1):1–24, 1972.

[31] Ryan T Canolty and Robert T Knight. The functional role of cross-frequency coupling. *Trends in Cognitive Sciences*, 14(11):506–515, 2010.

[32] John M Beggs and Dietmar Plenz. Neuronal avalanches in neocortical circuits. *Journal of Neuroscience*, 23(35):11167–11177, 2003.

[33] Janina Hesse and Thilo Gross. Self-organized criticality as a fundamental property of neural systems. *Frontiers in Systems Neuroscience*, 8:166, 2014.

[34] Enzo Tagliazucchi, Pablo Balenzuela, Daniel Fraiman, and Dante R Chialvo. Criticality in large-scale brain fMRI dynamics unveiled by a novel point process analysis. *Frontiers in Physiology*, 3:15, 2012.

[35] Giulio Tononi. An information integration theory of consciousness. *BMC Neuroscience*, 5(1):42, 2004.

[36] Masafumi Oizumi, Larissa Albantakis, and Giulio Tononi. From the phenomenology to the mechanisms of consciousness: integrated information theory 3.0. *PLoS Computational Biology*, 10(5):e1003588, 2014.

[37] Karl Friston. The free-energy principle: a unified brain theory? *Nature Reviews Neuroscience*, 11(2):127–138, 2010.

[38] Robin L Carhart-Harris, Robert Leech, Peter J Hellyer, Murray Shanahan, Amanda Feilding, Enzo Tagliazucchi, Dante R Chialvo, and David Nutt. The entropic brain: a theory of conscious states informed by neuroimaging research with psychedelic drugs. *Frontiers in Human Neuroscience*, 8:20, 2014.

[39] Adenauer G Casali, Olivia Gosseries, Mario Rosanova, Melanie Boly, Simone Sarasso, Karina R Casali, Silvia Casarotto, Marie-Aurélie Bruno, Steven Laureys, Giulio Tononi, and Marcello Massimini. A theoretically based index of consciousness independent of sensory processing and behavior. *Science Translational Medicine*, 5(198):198ra105, 2013.

[40] Yoshiki Kuramoto. Chemical oscillations, waves, and turbulence. *Springer Series in Synergetics*, 19, 1984.

[41] Wolf Singer. Neuronal synchrony: a versatile code for the definition of relations? *Neuron*, 24(1):49–65, 1999.

[42] Emmanuelle Tognoli and J A Scott Kelso. The metastable brain. *Neuron*, 81(1):35–48, 2014.

[43] David Attwell and Simon B Laughlin. An energy budget for signaling in the grey matter of the brain. *Journal of Cerebral Blood Flow & Metabolism*, 21(10):1133–1145, 2001.

[44] Tânia Tomé and Mário J de Oliveira. Entropy production in nonequilibrium systems at stationary states. *Physical Review Letters*, 108(2):020601, 2012.

[45] Udo Seifert. Stochastic thermodynamics, fluctuation theorems and molecular machines. *Reports on Progress in Physics*, 75(12):126001, 2012.

[46] Woodrow L Shew and Dietmar Plenz. The functional benefits of criticality in the cortex. *The Neuroscientist*, 19(1):88–100, 2013.

[47] Stanislas Dehaene and Lionel Naccache. Towards a cognitive neuroscience of consciousness: basic evidence and a workspace framework. *Cognition*, 79(1-2):1–37, 2001.

[48] Hans Berger. Über das Elektroenkephalogramm des Menschen. *Archiv für Psychiatrie und Nervenkrankheiten*, 87(1):527–570, 1929.

[49] Allan Rechtschaffen and Anthony Kales. *A Manual of Standardized Terminology, Techniques and Scoring System for Sleep Stages of Human Subjects*. UCLA Brain Information Service/Brain Research Institute, Los Angeles, 1968.

[50] Patrick L Purdon, Eric T Pierce, Eran A Mukamel, Michael J Prerau, John L Walsh, Kara FK Wong, Andres F Salazar-Gomez, P Grace Harrell, Aaron L Sampson, Aylin Cimenser, et al. Clinical electroencephalography for anesthesiologists: part I: background and basic signatures. *Anesthesiology*, 119(4):848–860, 2013.

[51] Nicholas D Schiff. Recovery of consciousness after brain injury: a mesocircuit hypothesis. *Trends in Neurosciences*, 33(1):1–9, 2010.

[52] Tadas Stumbrys, Daniel Erlacher, Melanie Schädl, and Michael Schredl. Induction of lucid dreams: a systematic review of evidence. *Consciousness and Cognition*, 21(3):1456–1475, 2012.

[53] Mikhail Belkin and Partha Niyogi. Laplacian eigenmaps for dimensionality reduction and data representation. *Neural Computation*, 15(6):1373–1396, 2003.

[54] Christian Wachinger, Polina Golland, William Kremen, Bruce Fischl, and Martin Reuter. BrainPrint: a discriminative characterization of brain morphology. *NeuroImage*, 109:232–248, 2015.

[55] Susan Pockett. The electromagnetic field theory of consciousness: a testable hypothesis about the characteristics of conscious as opposed to non-conscious fields. *Journal of Consciousness Studies*, 19(11-12):191–223, 2012.

[56] James M Shine. Neuromodulatory influences on integration and segregation in the brain. *Trends in Cognitive Sciences*, 23(7):572–583, 2019.

[57] Abraham Lempel and Jacob Ziv. On the complexity of finite sequences. *IEEE Transactions on Information Theory*, 22(1):75–81, 1976.

[58] Michael M Schartner, Robin L Carhart-Harris, Adam B Barrett, Anil K Seth, and Suresh D Muthukumaraswamy. Increased spontaneous MEG signal diversity for psychoactive doses of ketamine, LSD and psilocybin. *Scientific Reports*, 7:46421, 2017.